Leptospiral lipopolysaccharide dampens inflammation through upregulation of autophagy adaptor p62 and NRF2 signaling in macrophages

Delphine Bonhomme [1], Ignacio Santecchia [1], Pedro Escoll [2], Frédérique Vernel-Pauillac [1], Ivo G. Boneca [1] & Catherine Werts [1*]

[1] Institut Pasteur, Université Paris Cité, CNRS UMR6047, INSERM U1306, Unité de Biologie et Génétique de la Paroi Bactérienne, Paris, France

[2] Institut Pasteur, Université Paris Cité, CNRS UMR6047, Unité Biologie des Bactéries Intracellulaires, Paris, France

[*] corresponding author cwerts@pasteur.fr

ABSTRACT

Leptospira interrogans are pathogenic bacteria responsible for leptospirosis, a worldwide neglected zoonosis affecting yearly 1 million people. All vertebrates can be infected by leptospires. Some species like humans are susceptible to the disease whereas rodents such as mice are resistant and can even become asymptomatic renal carriers. Leptospires have been shown to avoid the activation of some innate immune receptors of the Toll-like receptors (TLRs) and NOD-like receptors families through their atypical microbe associated molecular patterns, and to escape some phagocyte functions. Autophagy is an essential nutrient-recycling cellular mechanism that is also crucial to clear invasive pathogens and is one of the many antimicrobial mechanisms that may be subverted upon bacterial infection. Here we showed that leptospires reduced the quantity of autophagosomes in murine and human macrophages. Moreover, leptospires infection induced a time-dependent specific accumulation of the autophagy adaptor p62 in puncta-like structures. Interestingly, we showed that these effects were not associated with an active leptospiral mechanism but were mediated by the recognition of the atypical leptospiral lipopolysaccharide (LPS) through TLR4 and TLR2. Moreover, we demonstrate in murine macrophages that leptospires induced, *via* p62 accumulation, the nuclear translocation of transcription factor NRF2, consequently triggering the retro-amplification of the p62/NRF2 axis. Finally, inhibition of p62/NRF2 signaling led to increased cytokines transcription and secretion. Overall, this suggests that the p62/NRF2 axis induced by leptospires contributes to dampening inflammation. These findings highlight a novel escape mechanism of leptospires, potentially participating in the stealthiness of the infection.

AUTHOR SUMMARY

Leptospira interrogans are pathogenic bacteria responsible for leptospirosis, a worldwide neglected zoonosis. Some species like humans may suffer from severe disease whereas rodents such as mice are asymptomatic renal carriers. Leptospires have been shown to escape different innate immune receptors of the host immune defenses, and largely escape phagocytosis. Autophagy is a host cell mechanism essential for nutrient-recycling but also crucial to fight and clear intracellular pathogens. Here we show by Western blot and automated microscopy, that infection with leptospires in human and murine macrophages did not trigger autophagy, although it triggered the specific accumulation of the autophagic adaptor p62. Interestingly, we show in murine macrophages that leptospiral infection also activated the nuclear translocation of the transcription factor NRF2. These effects were recapitulated with inactivated bacteria or using the leptospiral lipopolysaccharide (LPS). Finally, we show using RNA interference that inhibiting p62/NRF2 signaling led to increased inflammation. Overall, this suggests that the p62/NRF2 axis induced by the leptospiral LPS contributes to limiting the inflammation in macrophages. These findings highlight a novel mechanism of *Leptospira*, potentially contributing to their stealthiness.

INTRODUCTION

Leptospira interrogans are spirochete bacteria and the causative agent of leptospirosis, a worldwide neglected zoonosis that is currently reemerging because of climate change and causes around 60 000 deaths *per* year worldwide [1] Although all vertebrates can be infected by leptospires, they do not all present the same symptoms and susceptibility to the disease [2]. Humans as sensitive hosts may suffer from acute leptospirosis ranging from flu-like symptoms to potential multi-organ failure in 5-10% cases [1]. On the other hand, rodents such as mice and rats are resistant to acute illness and get chronically colonized upon infection [3]. Leptospires reach the proximal tubules in the kidneys and establish a stable colonization that leads to their excretion in the urine throughout the life of the animal, contributing to the spread of the zoonosis [3, 4].

The host immune defense relies on humoral and cellular components, such as the complement system, immunoglobulins, and phagocytes that patrol to fight microbes. Activation of immune cells such as macrophages are mediated by the sensing of microbial associated molecular patterns (MAMPs) by pattern recognition receptors (PRRs). Leptospires possess numerous lipoproteins, conferring them the ability to potently activate Toll-Like receptor 2 (TLR2) [5, 6]. However, they are stealth pathogens and escape recognition by several other PRRs through unique mechanisms. Our group showed that the leptospiral peptidoglycan escapes NOD receptors recognition by binding to LipL21, one of the numerous leptospiral lipoproteins [7]. We also showed that the leptospiral endoflagella escapes recognition by TLR5 [8]. Furthermore, previous studies on the leptospiral lipopolysaccharide (LPS), a virulence factor [9], revealed that the lipid A (lipidic anchor) possesses structural peculiarities [10] and that it does not activate the human TLR4 whereas it activates the murine TLR4. However, we recently showed that the recognition of the leptospiral LPS in murine macrophages is only partial, because the LPS escapes TLR4 endocytosis and subsequent activation of the TLR4-TRIF pathway [11]. We further demonstrated that the leptospiral LPS activates TLR2 [5], presumably through copurified lipoproteins such as LipL32 (the major leptospiral lipoprotein). On the other hand, our group also showed that leptospires activate the NOD-Like Receptors Pyrin 3 (NLRP) inflammasome and trigger IL1β production [12].

In addition to escaping recognition by several PRRs, leptospires also escape phagocytes' functions. Indeed, although leptospires are mostly extracellular bacteria, we reported that leptospires can be found within macrophages without intracellular replication, and that they evade killing by the classical microbicidal mechanisms such as xenophagy [13]. Autophagy is an essential mechanism allowing nutrient recycling upon starvation. Recently, xenophagy arose as a specific form of autophagy promoting the degradation of intracellular pathogens and dampening inflammation [14, 15]. Xenophagy has been shown essential to clear intracellular bacteria, such as *Mycobacterium tuberculosis*, *Shigella flexneri* and *Salmonella typhimurium* [16-18].

Autophagy induction is a tightly regulated process: upon stress, class III phosphoinositide 3-kinase (PI3K) complex (VSP34, Beclin-1, Atg14) promotes the nucleation of a double membrane called autophagophore [19]. In addition, ULK1/2 phosphorylates Atg13 to form the initiation complex [19]. The expansion of the phagophore is then possible *via* the Atg protein conjugation system [20]. Finally, the LC3 conjugation system is required to promote complete autophagosome formation. After translation, pro-LC3 proteins get cleaved (22 amino acids in C-ter) by protease Atg4 producing LC3-I. In turn, LC3-I gets conjugated by Atg7 (E1-like ligase) [21] and Atg3 that promote the addition of a phosphatidylethanolamine (PE) group [22]. The resulting LC3-II localizes on the membrane of the phagophore promoting its maturation in an autophagosome [23] and its fusion with lysosomes, hence leading to cargo degradation by lysosomal enzymes such as cathepsins. Although LC3-II of the inner leaflet will be degraded, LC3-II present in the outer leaflet will be recycled by Atg4, *via* de-lipidation and return to the LC3-I form [21]. Consequently, LC3-II turnover has been proposed as a good way to monitor autophagy [24].

Upon infection, several intracellular and extracellular immune signaling pathways can lead to autophagy induction. Toll-Like Receptors (TLRs) signaling facilitates autophagy through interaction of MyD88 complexes with Beclin-1 of the nucleation complex [15]. Furthermore, LPS recognition by TLR4 has been shown to be a potent activator of autophagy, *via* the endosomal TRIF pathway [25]. Other studies also demonstrated that NOD1 and NOD2 induce autophagy [26]. Given that leptospires escape both NODs and TLR4-TRIF pathways [7, 11], our study aimed to decipher the interplay between *L. interrogans* and the autophagy machinery of mouse macrophages. Therefore, we assessed autophagy by monitoring LC3-II, and autophagy adaptors, namely p62. Then, considering the importance of bacterial LPS in autophagy modulation [25], we investigated the potential role of the leptospiral LPS in autophagy modulation.

RESULTS

L. interrogans reduces the quantity of autophagosomes in macrophages

First, to assess the potential induction of autophagy by leptospires, we infected C57BL/6 mice with *L. interrogans* serovar Manilae (one of the most pathogenic serotypes) strain MFLum1 [4]. We injected intraperitoneally 5 x 10^7 leptospires/mouse and assessed LC3 levels in peritoneal cells by Western blot 4 h post-infection. Our results showed that leptospires did not trigger an increase in LC3-II levels, unlike injection of positive controls for autophagy induction: a mix of muropeptides, agonists of NOD1 and NOD2, or rapamycin (**Fig 1A**). Then, we infected bone marrow derived macrophages (BMDMs) *in vitro* with the same strain and monitored LC3-II 24 h post-infection. Here again, in contrast to autophagy induction triggered by rapamycin, we observed no increase in LC3-II after *Leptospira* infection (**Fig 1B**). The same observation was made upon stimulation with heat-killed

(HK) leptospires (**Fig 1B**). Furthermore, to address autophagy induction in cells from other vertebrate hosts, we infected human THP1 stably transfected with CD14 (hereafter THP1-CD14) with *L. interrogans* and monitored LC3-II by WB. Our results showed no accumulation of LC3-II after 4 h infection (**Fig S1**). Overall, these data showed that leptospires did not trigger autophagy in macrophages.

Second, to address potential modulation of the autophagy flux upon infection, we infected BMDMs with *L. interrogans* and then treated the cells prior to collection with Bafilomycin A1 (BafA1). BafA1 inhibits the fusion with lysosomes and arrests autophagy before degradation of cargo, including LC3-II, allowing the accumulation of autophagosomes and consequent analysis of the overall flux. Our results showed that there was an expected accumulation of LC3-II in BafA1 treated cells, but no major difference with or without infection, suggesting that leptospires do not alter the autophagy flux **(Fig 1C)**. To ensure that infection with leptospires did not modulate autophagy at earlier time points, we then performed kinetics analyses of LC3-II. Interestingly, we observed a slight yet robust time-dependent reduction of LC3-II levels 4 h and 24 h post-infection of BMDMs with *L. interrogans*, as evidenced by Western blot and their quantifications (**Fig 1D, lower panel**). Many bacteria interfere actively with autophagy functions via effectors or RNA interference [17, 27-32]. We therefore analyzed BMDMs after stimulation with HK leptospires and we observed similar LC3-II decrease over time (**Fig 1D, right panel**), excluding an active mechanism for LC3-II downregulation. To decipher the origin of LC3-II decrease upon infection, we infected BMDMs and analyzed LC3 mRNA levels by RT-qPCR 24 h post-infection. Our results showed that LC3 was not transcriptionally regulated upon infection with leptospires (**Fig 1E**), suggesting a post-transcriptional regulatory mechanism.

Last, to confirm this paradoxical LC3-II decrease despite no flux alteration upon infection, we used RAW-mLC3-DiFluo reporter cell line to specifically monitor autophagosomes and autolysosomes formation. These macrophages are stably transfected with LC3 tagged with tandem GFP-RFP. Both GFP and RFP fluoresce under basal conditions and when LC3 is embedded in the autophagosome membrane. However, when autophagosomes become autolysosomes, acidification of the environment quenches GFP fluorescence, and only RFP fluorescence remains. Using High-Content (HC) automated microscopy, we analyzed these cells 4 h post-infection with *L. interrogans*. Our results showed that both autophagosomes (RFP+GFP) and autolysosomes (RFP) were visible in the non-infected cells, and in the starved cells (EBSS) (**Fig 1F, white arrows**). Interestingly, and consistent with the Western blots results, we observed a decrease of the overall LC3-RFP fluorescence intensity upon infection as quantified at 4 h post-infection (**Fig 1G**). Unexpecttedly, we found by quantification of the number of autophagosomes and autolysosomes that leptospires triggered a decrease in autophagosome number, without altering the maturation to autolysosomes (**Fig 1G**). Here again, these results confirmed that leptospires did not block the autophagy flux while reducing the LC3-II autophagosomes structures.

L. interrogans induces specific accumulation of autophagy adaptor p62 in puncta-like structures

The adaptor proteins, such as Sequestosome 1 (SQSTM1, also known as p62), Nuclear Dot Protein 52 (NDP52) and optineurin (OPTN) [17, 33-36] are important players of xenophagy that allow selective bridging between the bacterial cargo and the autophagosome. The levels of these adaptors in the cells are regulated by autophagy: they are constitutively degraded upon lysosome / autophagosome fusion. Considering the LC3-II decrease induced by *L. interrogans*, we then addressed the consequences of the infection on the autophagy adaptors. We infected BMDMs with *L. interrogans* serovar Manilae strain MFLum1 and analyzed by Western blots the levels of the different adaptors. Strickingly, we observed a time-dependent accumulation of p62 upon infection (**Fig 2A**). We confirmed this phenotype upon infection of BMDMs with two other strains from pathogenic serotypes of *L. interrogans*: serovar Copenhageni strain Fiocruz L1-130 and serovar Icterohaemorrhagiae strain Verdun, and with the saprophytic *Leptospira biflexa* serovar Patoc strain Patoc I (**Fig 2B**). Such accumulation of the adaptor p62 could have been non-specifically associated with the reduction of autophagosomes. However, while performing infection of RAW264.7 cells, we observed no difference in the levels of other adaptors OPTN and NDP52 upon infection (**Fig S2A**). We concluded that *L. interrogans* triggered specific accumulation of p62 in murine BMDMs.

To investigate the specific mechanism of p62 accumulation triggered by leptospires, we analyzed the transcriptional regulation of p62 upon infection by RT-qPCR. In BMDMs infected with *L. interrogans*, we observed a significant upregulation of p62 mRNA 24 h post-infection (**Fig 2C**). This corroborated the idea that p62 accumulation is not only mediated by autophagy downregulation. Furthermore, we also analyzed infected BMDMs by fluorescence microscopy and we observed that, 4 h post-infection, p62 accumulated in puncta-like structures (**Fig 2D**). The kinetics of these p62 puncta formation were further characterized using automated HC confocal microscopy. Upon infection of RAW264.7 cells by *L. interrogans*, we quantified the number of p62 puncta *per* cell, as well as the percentage of cells with p62 puncta. Results showed time-dependent increase of both p62 puncta *per* cell and percentage of positive cells and showed around 80% of cells positive for p62 with an average of 6 puncta *per* cell 24 h post-infection (**Fig 2E**). Similar analyses were performed after infection with *L. biflexa*, confirming a higher p62 puncta formation with the saprophytic strain, compared to the pathogenic Manilae (**Fig S2B**). Such findings were confirmed by single cell analysis of RAW264.7 cells infected with *L. interrogans*, that showed an average of 5-10 puncta *per* cell with some macrophages containing up to 60 p62 puncta (**Fig 2F**). Of note, BafA1 that prevents the acidification of lysosomes and consequently blocks autophagy flux also led to p62 accumulation, but to a much lower extent than infection with leptospires (**Fig 2E and 2F**).

Finally, considering the host species-specificity of different escape mechanisms triggered by leptospires, we also addressed in human cells the effect of infection on p62. Therefore, we infected

THP1-CD14 cells with *L. interrogans* serovar Manilae strain MFLum1. We also observed a specific p62 accumulation and no NDP52 accumulation after infection with leptospires (**Fig S2C**), suggesting a conserved mechanism in human and murine macrophages.

Autophagy modulation is mediated by TLR2/TLR4

Considering that leptospires did not reduce LC3-II levels through an active mechanism, we then addressed the role of PRRs in autophagy modulation. Since leptospires are potent agonists of TLR2 and signal through TLR4-MyD88 in murine cells [11], we analyzed autophagy modulation in macrophages lacking both TLR2 and TLR4. To do so, we infected wild-type (WT) and TLR2/TLR4 double knock-out (TLR2/4 dko) BMDMs with *L. interrogans.* After 24 h of infection, we assessed by Western blot the levels of LC3-II and p62. Our results showed that, in contrast to WT cells, there was no reduction in LC3-II and no accumulation of p62 in TLR2/4 dko BMDMs (**Fig 3A**), suggesting that autophagy modulation by leptospires is mediated by these two receptors. To further confirm such results, we also infected WT and MyD88/TRIF dko macrophages, that lack both adaptors for TLRs signaling. Here again, we observed no accumulation of p62 in MyD88/TRIF BMDMs compared with the WT BMDMs (**Fig 3B**).

Finally, we investigated the role of TLR2/TLR4 in the specific accumulation of p62. We first analyzed infected BMDMs by RT-qPCR and observed that the increase in p62 mRNA levels observed in WT BMDMs was abolished in TLR2/4 dko BMDMs (**Fig 3C**). Furthermore, we performed single cell analysis of p62 puncta formation in WT, TLR2/4 dko and MyD88/TRIF dko BMDMs upon 24 h infection by three serotypes of *L. interrogans* (serovar Manilae strain L495, serovar Copenhageni strain Fiocruz L1-130 and serovar Icterohaemorrhagiae strain Verdun). Our results showed that the number of p62 puncta *per* cell was greatly reduced in TLR2/TLR4 dko cells and almost completely abolished in MyD88/TRIF dko cells (**Fig 3D**), which may suggest the involvement of other TLRs than TLR2 and TLR4s in the leptospiral p62 upregulation.

Given that leptospires modulate autophagy in a TLR2/TLR4 dependent manner, we finally addressed the potential role of inflammasome in autophagy dampening. Indeed, leptospires have been shown to activate NLRP3 in a TLR2/TLR4-dependent manner [12], and NLRPs inflammasomes have been shown to modulate autophagy [37-40]. We therefore stimulated BMDMs with both live and heat-killed leptospires in presence or absence of glibenclamide, a NLRP3 inhibitor. We first confirmed the efficiency of the treatment by measuring IL1β production after 24 h, as a readout for inflammasome activation. Our result showed that IL1β was produced upon infection by leptospires, but reduced in presence of glibenclamide, confirming that glibenclamide inhibited NLRP3 (**Fig S3A**). We then analyzed by Western blot the levels of LC3-II, and we observed a reduction of LC3-II upon infection with either live or heat-killed leptospires in both control and glibenclamide treated cells (**Fig S3B**).

This suggests that the modulation of autophagy by leptospires, although TLR2/TLR4 dependent, is not mediated by activation of NLRP3 inflammasome.

p62 accumulation is mediated by the leptospiral LPS

With the predominant role of TLR2 and TLR4 in autophagy modulation, and transcriptional regulation of p62, we then hypothesized that these effects could be induced by the leptospiral LPS. To address the role of the leptospiral LPS in the p62 accumulation phenotype, we first infected BMDMs with both heat-killed leptospires (recapitulating MAMPs) and purified leptospiral LPS. Western blot analyses showed that p62 got accumulated in a time-dependent manner in response to both heat-killed leptospires and also 24 h post-stimulation with their LPS (**Fig 4A**). We further characterized by HC microscopy the kinetics of p62 puncta formation in BMDMs after incubation with live, heat-killed *L. interrogans* serovar Manilae strain L495 and purified LPS. Results indicated that LPS stimulation induced the exact same p62 puncta formation than the one observed with bacteria (**Fig 4B**). Next, we also analyzed BMDMs at the single cell level 24 h post-infection. Here again, HK leptospires or the leptospiral LPS were sufficient to recapitulate p62 puncta formation in cells (**Fig 4C**). Overall, our results showed that p62 accumulation was mediated by the leptospiral LPS.

Leptospiral LPS also triggers translocation of NRF2 transcription factor

When autophagy adaptors accumulate in cell (in the absence of functional autophagy or because of specific upregulation), stress pathways are induced. For instance, p62 accumulation has been shown to induce translocation of stress-responsive nuclear factor erythroid 2-related factor 2 (NRF2) [41-43]. Subsequently, NRF2 triggers antioxidant and anti-apoptotic programs [41, 42], and promotes p62 upregulation, creating a loop that counteracts stress in autophagy-deficient conditions [41]. We therefore infected BMDMs with *L. interrogans* serovar Manilae strain L495 and analyzed NRF2 by immunofluorescence 4 h post-infection. Results showed that NRF2 staining was barely visible in the non-infected conditions, whereas NRF2 was visible in the nucleus of cells upon infection (**Fig 5A**). This suggests that leptospires triggered NRF2 translocation in murine macrophages. Interestingly, we also observed that not all macrophages seem activated to the same extent (**Fig 5A**). Then, we decided to perform single cell analysis of NRF2 fluorescence intensity in the nucleus of cells infected with three different serovars of *L. interrogans.* Similarly, upon infection, the levels of NRF2 fluorescence in the nucleus increased (**Fig 5B**). Next, we calculated the ratio of NRF2 intensities [nucleus/cytoplasm] and estimated that cells positive for NRF2 had a ratio > 1.4. We then plotted the percentage of cells with NRF2 ratio superior to 1.4 and observed that up to 60% of cells were positive after 4 h of infection (**Fig 5C**). Finally, we addressed the role of the leptospiral LPS and performed similar analyses on BMDMs stimulated for 4 h with either live, heat-killed leptospires or their purified

LPS. All conditions triggered similar NRF2 translocation (**Fig 5D and 5E**), suggesting that the leptospiral LPS is responsible for NRF2 activation.

p62 and NRF2 constitute a retro-activation loop upon infection with *L. interrogans*

Consequently to p62 accumulation and NRF2 translocation upon infection with *L. interrogans*, we investigated the potential regulation mechanisms between these two phenotypes. Thus, we performed small-interfering RNA (siRNA) transfection in BMDMs to knock-down specifically p62 or NRF2. We then infected the transfected BMDMs and analyzed NRF2 and p62 4 h post-infection by HC microscopy. First, we analyzed the NRF2 ratio [nucleus/cytoplasm] during p62 knocking-down. Our results showed that NRF2 ratio was lower in p62 siRNA condition (**Fig 6A**). Absence of p62 was confirmed and quantified by confocal microscopy (**Fig 6B**). Conversely, we then analyzed p62 puncta formation upon NRF2 siRNA treatment. Our results showed that p62 puncta formation was altered in NRF2 siRNA conditions (**Fig 6C**). Similalrly, NRF2 knocked-down was confirmed and quantified (**Fig 6D**). Overall, these results showed that p62 contributed to NRF2 translocation, and that, in turn, NRF2 regulated p62 puncta formation, suggesting that p62 and NRF2 are in a retro-activation loop upon infection by *L. interrogans*.

To further characterize the involvement of NRF2 in p62 retro-activation, we analyzed BMDMs transfected with NRF2 siRNA and infected with *L. interrogans* by Western blot and RT-qPCR 24 h post-infection, allowing us to measure both the protein and mRNA levels of p62. Interestingly, we observed that NRF2 silencing prevented p62 protein accumulation (**Fig 6E**) but also reduced mRNA upregulation (**Fig 6F**), suggesting that NRF2 contributes transcriptionally to p62 retro-activation.

NRF2 translocation prevents inflammation upon infection

NRF2 is a stress response transcription factor that promotes antioxidant and antiapoptotic programs upon activation [41, 42]. Therefore, we first monitored the transcription of targets genes involved in fighting oxidative stress in macrophages in response to infection. We infected BMDMs with *L. interrogans* and analyzed by RT-qPCR the levels of gluthatione S-reductase and catalase mRNA at 4 h and 24 h post-infection. Surprisingly, we observed no upregulation of these transcripts (**Fig S4A and S4B**), suggesting that no antioxidant program is activated upon infection with *L. interrogans*.

Interestingly, NRF2 was shown to also have repressor functions and to dampen inflammation by inhibiting the transcription of cytokines [44, 45], hence conferring resistance to inflammatory disease such as sepsis [44]. We therefore investigated the role of NRF2 translocation in inflammation upon infection by leptospires. We transfected RAW624.7 cells with siRNA targeted against NRF2 and then infected them with *L. interrogans*. First, we observed a decrease in macrophage viability upon infection of NRF2-silenced cells (**Fig 7A, left panel**), as expected considering that NRF2 is known to

prevent cell death. Interestingly, this enhanced loss of viability was not associated with lactate dehydrogenase (LDH) release from the cytosol, illustrating that no membrane damage or cell lysis was occurring (**Fig 7A, right panel**). We then analyzed the mRNA levels of several cytokines and enzymes, namely iNOS (nitric oxide inducible synthase), IL6, TNF and IL10. Upon infection, all mRNA levels were higher in NRF2-silenced cells than in control cells (**Fig 7B**), suggesting that NRF2 does play a role in repressing the expression of inflammatory targets. Finally, to address whether this transcriptional regulation was strong enough to alter cytokines levels, we analyzed nitric oxide (NO), IL6, TNF and IL10 production in cell supernatant. Consistent with the mRNA analyses, we observed higher NO, IL6 and TNF upon infection of NRF2-silenced RAW264.7 (**Fig 7C**). Interestingly, IL10 levels were not modulated in NRF2-silenced cells. All these findings were even more striking when normalizing the cytokines production with the cell viability (**Fig 7C, grey area**). Overall, NRF2 played a repressor role to dampen NO, TNF and IL6 production in mouse macrophages upon infection with *L. interrogans*.

DISCUSSION

Our results showed that *L. interrogans* does not induce autophagy in macrophages either *in vivo* in mice or *in vitro* in murine and human cells. These findings are consistent with previous studies from our laboratory showing that leptospires escape NOD1/NOD2 [7] and TLR4-TRIF [11] activation, since both pathways have been described as autophagy inducers [25, 26]. Furthermore, infection with leptospires unexpectedly triggered a slight reduction of the number of autophagosomes, without alteration of the autophagy flux. To this date, we do not know what the functional consequences of such downregulation are, warranting further investigations. Interestingly, using heat-killed leptospires we observed similar results, excluding a potential active mechanism. We conclude that the leptospires behave differently from other pathogenic bacteria such as *Legionella pneumophila*, *Shigella flexneri* or *Listeria monocytogenes* for which autophagy modulation is mediated by effector proteins, namely RavZ, IcsB and ActA respectively [31, 32]. An effector-independent mechanism is even more consistent with the fact that leptospires do not possess traditional secretion systems (SS) such as type-III SS or type-IV SS. Indeed, only the presence of an incomplete type-II SS has been identified in *Leptospira* species [46]. Consistently, a study revealed that 59% of the pathogen-specific leptospiral genes have unknown functions, strongly suggesting that the leptospiral virulence may rely on unique and novel mechanisms [3]. Our results further showed that the modulation of autophagy was induced by leptospiral LPS signaling through TLR2/TLR4. The unique leptospiral LPS, the best characterized virulence factor [9], plays an important role in leptospiral host-pathogen interactions. Indeed, we previously showed that leptospiral LPS avoids human TLR4 and mouse TLR4-TRIF activation. Recently, through the atypical structures of its lipid A and O antigen [11, 47, 48], LPS has also been shown to prevent cell death by pyroptosis.

Therefore, it was not surprising to attribute the autophagy modulation phenotype to leptospiral LPS. Interestingly, the LPS of *L. biflexa* was shown to be a more potent TLR4 agonist [11], potentially explaining the stronger p62 accumulation observed after infection with the saprophytic strain.

TLRs signaling has classically been associated to autophagy induction, mainly through TLR4-TRIF [25] but also *via* TLR2, TLR3, TLR4, TLR5 and TLR7 signaling with MyD88 [15]. However, consistent with our results, some studies also reported that TLRs signaling can also block autophagy. For instance, LPS signaling downregulates autophagy in non-inflammatory dendritic cells (DCs) [49] and in microglial cells [50], evidencing the complexity of the autophagy/TLR interplay. In DCs, TLR4 has been associated with mTOR activation, hence reducing the autophagy flux [49]. Whether this mechanism could also be used by leptospires in macrophages remains to be answered. In addition, leptospires have been shown to induce NLRP3 in a TLR2/TLR4-dependent manner [12]. Although the interplay between NLRP3 and autophagy is unclear, several studies reported that NLRP3 can dampen autophagy [37-40]. Therefore, we hypothesized that *Leptospira*-induced NLRP3 could modulate autophagy. However, our results suggest that the NLRP3 does not contribute to the autophagy modulation.

A consequence of autophagy downregulation is the accumulation of a central player of the autophagy pathway, the p62/SQSTM-1 adaptor [43]. This protein has been shown to accumulate *via* TLRs signaling [51], most likely through NFκB-mediated transcriptional regulation. Our results showed that TLR2/TLR4 control the accumulation of p62 upon infection by leptospires. Nevertheless, we cannot differentiate a direct mechanism (NFκB) from an indirect one (autophagy dysregulation). Our data showing that p62 is transcriptionally regulated led us to favor the first hypothesis. Moreover, the levels of p62 upon infection are higher than after BafA1 treatment, suggesting that the accumulation of p62 is mostly independent of the slight autophagy downregulation induced by leptospires.

The TLRs-induced accumulation of p62 has been shown to trigger the translocation of the transcription factor NRF2 [51]. Under physiological conditions, NRF2 is classically targeted for degradation by the proteasome *via* interaction with its inhibitor Keap1 [43, 52]. The accumulation and direct binding of p62 to Keap1, leads to its sequestration and subsequent release from NRF2, which then can translocate in the nucleus [41-43, 52]. Our results confirmed that p62 induces translocation of NRF2 upon infection with leptospires. Other microbes such as Epstein-Barr virus (EBV) or parasite *Leshmania major* have been shown to activate the p62/NRF2 axis [53, 54], hence showing an important role of NRF2 in response to pathogens. However, to date, the role of NRF2 translocation in response to pathogens remains unclear.

We then illustrated that the retro-activation loop between p62 and NRF2, described in the literature [41], is activated upon *L. interrogans* infection. Our results showed that p62 accumulation

triggered translocation of NRF2 and that in turn, NRF2 contributed to the transcriptional regulation of p62. Interestingly, this loop has few negative regulators, and it is hypothesized that its main regulator would be autophagy, through degradation of p62 [41]. However, considering the lack of autophagy induction upon infection with leptospires, it is not surprising that the loop remains active and that p62 puncta did not disappear even at 24 h post-infection. This suggests that leptospires are potent activators of the p62/NRF2 axis in macrophages.

NRF2 is involved in numerous pathways including the induction of antioxidant programs [41]. We were therefore surprised to observe no modulation in the mRNA levels of antioxidant targets, such as catalase or gluthatione S-reductase, either at 4 h or 24 h post-infection. Of note, pathogenic leptospires are equipped to fight against oxidative stress with inducible catalase, peroxidase, and peroxiredoxin [55]. We therefore hypothesize that leptospires would not benefit from induction of antioxidant program in the host cells. Interestingly, active repression of these NRF2-dependent antioxidant targets was previously shown upon infection with live *Leshmania major* parasite [54, 56] Whether leptospires could also actively prevent upregulation of NRF2 antioxidant targets remains to be addressed.

Alternatively, NRF2 has been shown to have transcription inhibition properties. Indeed, in BMDMs, NRF2 was described as an inhibitor of transcription for pro-inflammatory targets such as IL6, IL1β and IL12 [45, 57]. Our results showed that this was also the case upon infection with *L. interrogans.* Accordingly, we did not observe dampening of the anti-inflammatory IL10 upon infection. NRF2 inhibits polymerase III recruitment and hence prevents transcription of cytokines in response to stimulation [45]. Consequently, NRF2 was shown to downregulate neutrophils activation and migration [58]. Interestingly, neutrophils are barely observed in tissues of mice and humans infected with leptospires, although they are found in numbers in blood [59, 60]. Whether NRF2 translocation in specific cell type could have a role in this phenotype remains to be studied. NRF2 was also associated to inflammation reduction *via* indirect mechanism relying on STING and type I IFN downregulation [61], which remains to be studied in the case of leptospiral infection.

Finally, we showed that accumulation of p62 observed in murine macrophages was conserved in human cells. Although we could not address NRF2 translocation in human cells due to lack of specific antibodies and tools, we may speculate that inflammation dampening could therefore be conserved in human macrophages. Although the functional consequences of this mechanism remain to be addressed, we believe it could play a key role in the discretion of leptospires in hosts, lack of immune cell recruitment and potentially contribute to the establishment of chronic infections.

MATERIALS AND METHODS

***Leptospira interrogans* cultures.** *Leptospira interrogans* used in this work (serovar Manilae strain L495 and bioluminescent derivative MFLum1 [4], serovar Copenhageni strain Fiocruz L1-130, serovar Icterohaemorragiae strain Verdun) and *Leptospira biflexa* (serovar Patoc strain Patoc I) were grown in Ellinghausen-McCullough-Johnson-Harris (EMJH) medium at 28°C without agitation and diluted weekly, or twice a week for *L. biflexa*, to obtain exponential phase growth culture at the time of experiments. For infection, leptospires cultures were centrifuged (3250 g, 25 min), resuspended in endotoxin-free PBS (Lonza), enumerated using a Petroff-Hauser chamber and bacterial concentration was adjusted accordingly. To inactivate bacteria (thereafter called "heat-killed") leptospires were heated at 56 °C for 30 min with mild agitation. For fluorescent labelling, 10 mL of exponential culture was centrifuged (3250 g, 25 min) and the pellet was resuspended in the same volume of PBS (Lonza) with addition of 10 µM CFSE (Sigma). The bacterial suspension was incubated at room temperature for 30 min protected from light and washed 1 time with 20 mL of PBS before counting and infection.

Mice experiments. Adults male and female mice of the following genotypes in a C57/BL6 background were used: WT (Janvier Labs, Le Genest-Saint-Isle, France); TLR2$^{-/-}$TLR4$^{-/-}$ and MyD88$^{-/-}$/TRIF^{lps2} (both from Institut Pasteur). For peritoneal cavity analyses, mice were injected *via* intraperitoneal route with 5 x 10^{7} leptospires/mouse, 30 µg/mouse of rapamycin (Sigma) or 30 µg/mouse of NOD1 agonist (FK156) [62] and NOD2 agonist (MDP, Invivogen) in PBS. Next, 4 h post-infection mice were euthanized, and peritoneal content was recovered as previously described [63]. Briefly, skin was peeled and clamped, followed by the injection of 2 mL of RPMI media. Next an incision was made on the pre-clamped skin to recover the peritoneal content. Peritoneal cells were then used for sample preparation and Western blot analyses, as described below.

Ethic statement. All protocols were undertaken in compliance with EU Directive 2010/63 EU and the French regulation on the protection of laboratory animals issued on February 1st, 2013. They are part of projects approved by the Institut Pasteur ethics committee for animal experimentation (Comité d'Ethique en Expérimentation Animale CETEA registered under #89) under # HA0036 for the bone marrow cells, and #2014-0049 for the leptospiral infections, which was authorized by the French Ministry of Research, the French Competent Authority under #8562.

Cell culture. RAW264.7 murine macrophage-like cell line was cultured in complete RPMI containing glutamine (Lonza) and supplemented with 10 % v/v heat-inactivated fetal calf serum (HI-FCS, Gibco), 1 mM non-essential amino acids (MEM, Gibco) and 1 mM sodium pyruvate (NaPy, Gibco). RAW-mLC3-DiFluo (Invivogen) autophagy reporter cells stably transfected with LC3-GFP-RFD were cultivated in the same conditions, with the addition of 100 µg/mL zeocin (Invivogen) for efficient selective pressure. All the cells were seeded in 96-, 24-, 12-well plates (TPP) the day before

infection at a concentration of $0{,}3x10^6$ cells/mL in 200 µL, 1 mL or 2 mL respectively, in antibiotic-free medium.

Human THP-1 monocyte-like cell line, stably transfected with CD14 (THP1-CD14), was culture in complete RPMI, and the cells were differentiated for 48 hours with 20 ng/mL of phorbol 12-myristate 13-acetate (PMA, Invivogen) at $1x10^6$ cells/mL. The cells were then washed 3 times with PBS and allowed 24 hours of resting before infection.

BMDMs were obtained from different genotypes of C57BL/6 background mice. After euthanasia by cervical dislocation, the head of each bone was removed, and 2 mL of medium were passed through the bones using a 22 G needle to flush out the bone marrow. Bone marrow cells were centrifuged (300 g, 7 min) and treated with Red Blood Cell Lysis Buffer (Sigma-Aldrich) for 10 minutes, followed by another centrifugation. The cells were then enumerated, and $5x10^6$ cells were seeded in 100 cm^2 cell culture dishes in 12 mL of complete RPMI supplemented with 10% v/v L929 cell supernatant and 1x PenStrep (Gibco). Cells were incubated at 37 °C, 5 % CO_2. At day 3, 3 mL of the same medium was added. At day 7, the cells were collected by scraping in Cell Dissociation buffer (Gibco), centrifuged, enumerated, and seeded for infection at $1x10^6$ cells/mL.

In addition to the infections with *L. interrogans*, other treatments were performed. Starvation was induced in minimum EBSS media (Gibco) after 2 washes to remove complete cell culture media. Autophagy was induced with 500 mM rapamycin (Sigma). For blockage of autophagy flux, 100 nM bafilomycin A1 (BafA1, Sigma-Aldrich) was added to the infected cells 4 h before cell collection and analyses. The inflammasome inhibitor glibenclamide (Thermo Fisher) was added at 25 µM, 30 min before infection. Finally, stimulations by leptospiral LPS were performed by incubating the cells with 1 µg/mL of LPS of *L. interrogans* (serovar Manilae strain L495, serovar Copenhageni strain Fiocruz L1-130 or serovar Icterohaemorragiae strain Verdun) extracted from the phenol phase of the hot water/phenol extraction protocol, as we recently reviewed[64].

Immunofluorescence and High Content (HC) microscopy. For classical IF analyses, cells were seeded in 24-well plate containing 1 cover glass per well (18 mm diameter, # 1.5 thickness, Electron Microscopy Science). After infection, cells were fixed in 4 % v/v *para*-formaldehyde for 10 min, followed by three washes with PBS. Cells were blocked 1 h in PBS with 2.5% w/v bovine serum albumin (BSA) and 2.5 µg/mL anti-CD16-CD32 (FcBlock, Thermo Fisher). Cells were stained after blocking with primary antibodies (**Table 1**) overnight at 4 °C in PBS 1% w/v BSA, 0.05% w/v saponin. Cells were then washed three times with PBS and were incubated with fluorescent secondary antibodies (**Table 1**) and 1µg/mL DAPI in PBS 1% w/v BSA, 0.05% w/v saponin for 1 hour at room temperature. For NRF2 nuclear staining, permeabilization was initially performed by 10 min incubation in PBS 1% w/v BSA, 0.5% v/v Triton X-100 prior to blocking, and saponin was not used. In all cases, cells were washed three times with PBS and image acquisition was performed on Leica

SP5 confocal microscope (63x - 1.4 NA, oil immersion). Default settings were used and both UV and argon lasers were used at power between 5-40 %.

For HC microscopy analyses, cells were seeded in dark, transparent bottom 96-well plates (Greiner, µClear) at $0{,}1x10^6$ cells/mL. Staining protocols are identical to the ones described above, except for RAW-mLC3-DiFluo cells that were fixed to 10 min in cold ethanol/acetone (1:1) buffer. All cells were then kept in PBS for imaging by Opera Phenix HCS (Perkin Elmer) using confocal settings with a 63X water-immersion objective (NA 1.15). Light source was kept at 20 to 50% power and exposure time was set for each experiment to obtain intensities around 1000-5000. Automated acquisition was launched to acquire a minimum of 500-1000 cells/well in technical triplicates for each experiment. Automated image analysis workflow and puncta quantification was performed using Columbus image data storage and analysis system (PerkinElmer), with the following steps: *(i)* import data; *(ii)* find nuclei with DAPI signal; *(iii)* find cytoplasm with the background of the target protein signal (NRF2 or p62); *(iv)* find spots using method C if relevant (for p62); *(v)* formulate classical outputs: number of p62 puncta, NRF2 intensity in nucleus/cytoplasm; *(vi)* formulate calculated outputs: %p62 positive cells, NRF2 ratio, %NRF2 positive cells*; (vii)* save script and run batch analysis and *(viii)* export data.

Table 1. Antibodies list for immunofluorescence and Western blot analyses

Application*	Target	Clonality**	Conjugated	Host	Dilution	Reference	Supplier
IF	**p62**	mAb	Purified	Rabbit	1:500	ab109012	Abcam
	Rabbit IgG	pAb	AlexaFluor 488	Goat	1:1.000	A-11034	ThermoFisher
IF	**Nrf2**	mAb	Purified	Rat	1:250	#14596	CST
	Rat IgG	pAb	AlexaFluor 647	Goat	1:1.000	A-21247	ThermoFisher
WB	**LC3**	pAb	Purified	Rabbit	1:1.000	L7543	Sigma
	p62	mAb	Purified	Mouse	1:1.000	ab109012	Abcam
	OPTN	pAb	Purified	Rabbit	1:1.000	ab23666	Abcam
	NDP52	pAb	Purified	Rabbit	1:1.000	GTX115378	GeneTex
	Rabbit IgG	pAb	HRP	Goat	1:10.000	7074S	CST

* IF: immunofluorescence, WB: Western blot, ** mAb: monoclonal antibody, pAb: polyclonal antibody

SDS-PAGE and Western blot. For proteins collection and Western blot analyses, cell supernatants were removed, and 1 mL of Cell Dissociation buffer (Gibco) was added and incubated for 5 minutes, followed by scrapping, collection, and centrifugation (400 g, 10 min, 4 °C). The pellets were resuspended in 50 µL of ice-cold RIPA lysis buffer supplemented with 1x complete Mini, EDTA-free proteases inhibition cocktail (Roche). Cells were lysed on ice for 20 min followed by a centrifugation step (12000 g, 40 min, 4 °C) to remove the non-soluble material. Proteins were dosed using the Bradford assay and the samples were denatured in Laemmli buffer (99 °C, 10 min). SDS-PAGE was

done using 4-15% gradient acrylamide Stain-free gels (BioRad), loaded with 5-10 µg of protein extract *per* lane and gels were run at 100 V in Tris-Glycine-SDS buffer (BioRad). Proteins were visualized using stain free reagent in ChemiDoc (BioRad) with a 5 min exposition time and transferred onto a 0.22 µm PVDF membrane (BioRad) using Mixed MW fast transfer of 1 miniGel (BioRad). The membrane was blocked with 5% BSA in TBS with 0,05% v/v Tween 20 (TBS-T) for 60 minutes at room temperature with mild agitation. The membrane was probed with either anti-LC3 or anti-p62, anti-NDP52, anti-OPTN (**Table.1**) in 5% BSA in TBS-T overnight at 4 °C. The membranes were then washed in TBS-T 3 times for 15 minutes followed by incubation with secondary anti-rabbit IgG HRP-linked (**Table 1**) in 5% BSA in TBS-T for 60 minutes protected from light at room temperature, followed by 3 washes in TBS-T for 15 minutes. Blots were revealed using the Clarity reagent (BioRad) with automatic exposure time. Western blot quantifications were performed using Image Lab software (BioRad), and LC3-II levels were quantified after normalization by the strain free (total amounts of proteins/lane).

Small interfering RNA transfection. For siRNA transfection, cells were seeded at confluence of $0{,}1 \times 10^6$ cells/mL in 24-well plate (TPP) the day before transfection. In each well, transfection was performed using 4,5 µL of Lipofectamine siRNA Max reagent (ThermoFisher) in 650 µL of OptiMEM media (Gibco) and according to the manufacturer's instructions. The final concentration of commercial predesigned siRNA targeting *p62* and *nrf2* (FlexiTube, Qiagen) was 80 nM and the corresponding scramble siRNA (all start negative, Qiagen) was performed as control. The siRNA preparations in lipofectamine were incubated at room temperature for 25 min before delicate transfection of the cells. After 12 hours, 350 µL of complete RPMI was added on the cells. The infection was performed 24 hours post-transfection in complete RPMI and the reduction in p62 and NRF2 levels was checked by HCS microscopy.

ELISA and Griess reaction. Fresh cell culture supernatants were used 24 h post-infection for dosage of nitric oxide (NO) by the Griess reaction. On the other hand, cytokine dosage was performed on frozen supernatants by ELISA using DuoSet kits (R&D Systems), according to the manufacturer's instructions.

Viability and LDH release assays. LDH release was measured using the CyQuant LDH Cytotoxicity Assay kit (fresh supernatant) (Invitrogen), according to the manufacturers' instructions. On the other hand, viability was measured using MTT assay: after infection, cells were incubated for 2 h in 1 mg/mL MTT solution (Sigma) in complete RPMI. MTT crystals were then dissolved in HCl 1 M, isopropanol (1:24) and absorbance was read at 595 nm.

RT-qPCR. RNAs were extracted from frozen cells using RNeasy Mini Kit (Qiagen) according to the manufacturer's instructions. cDNAs were then obtained by retro-transcription (RT) using SuperScript II RT (Invitrogen). The equivalent of 20ng of cDNA were used for RT-qPCR with

specific primers and probes (**Table 2**). qPCR was performed using Taqman Universal MasterMix (Applied Biosystems) on a StepOne Plus Real Time PCR System (Applied Biosystems) with the standard protocol. Fold changes were calculated with the $2^{-\Delta\Delta Ct}$ method, using hypoxanthine guanine phosphoribosyl transferase (HPRT) as internal control.

Table 2. Primers and probe list for RT-qPCR analyses

Target	Forward primer sequence	Reverse primer sequence	Probe sequence
p62	5'-ATGTGGAACATGGAGGGAAGAG-3'	5'-TTCTGTGCCTGTGCTGGAACT-3'	5'-CCGCCTGACACCCACTACCCCA-3'
lc3	5'-GCCCCACCCCTGAAAGG-3'	5'-TGCAGAGGAAATGACCACAGAT-3'	5'-TGGCTCCCCTTGTCCTGACTCGG-3'
iNOS	5'-CATGACTGCTAATGTCAGAG-3'	5'-TCCTAGTCCATCCGGATAAA-3'	5'-GAAATCTGAGTTTGGCCTGAGG-3'
tnf	5'-CATCTTCTCAAAATTCGAGTGACAA-3'	5'-TGGGAGTAGACAAGGTACAACCC-3'	5'-CACGTCGTAGCAAACCACCAAGTGGA-3'
il6	5'-CTCCAGCTTATCTGTTAGGA-3'	5'-CTTCAACCAAGAGGTAAAAGA-3'	5'-AAATTGGGGTAGGAAGGACTATTTTATG-3'
il10	5'-GGCGCTGTCATCGATTTCTC-3'	5'-GACACCTTGGTCTTGGAGCTTATTAA-3'	5'-AAAATAAGAGCAAGGCAGTGGAGCAGGTG-3'
hprt	5'-CTGGTGAAAAGGACCTCTCGA-3'	5'-TGCCCTTGACTATAATGAGTACTTCA-3'	5'-TGTTGGATACAGGCCAGACTTTGTTGGAT-3'
cat	Pre-designed: Mm00437992_m1 (ThermoFisher)		
gsr	Pre-designed: Mm01197925_m1 (ThermoFisher)		
hprt	Pre-designed: Mm03024075_m1 (ThermoFisher)		

Statistical analyses. All statistical analyses were performed using Student's *t*-test with corresponding *p* values: * for $p < 0.05$; ** for $p < 0.01$ and *** for $p < 0.001$.

ACKNOWLEDGMENTS

We acknowledge Nathalie Aulner and Anne Danckaert (Institut Pasteur) as well as the Photonic BioImaging Unit of Technology and Service, a member of the France-BioImaging infrastructure, for support in conducting this study.

FUNDING

This work was funded by Institut Pasteur grant PTR2017-66 to CW and by Agence Nationale de la Recherche (ANR) grant ANR-10-LABX-62-IBEID to IGB. DB was funded by Université Paris Cité (formerly Université Paris Diderot) through Doctoral school FIRE (ED FIRE474). IS has been part of the Pasteur-Paris University (PPU) International PhD program. This program has received funding from the Institut Carnot Pasteur Microbes & Santé, and the European Union's Horizon 2020 research and innovation program under the Marie Sklodowska-Curie grant agreement no. 665807. IS has additionally benefited from a scholarship "Fin de thèse de science" number FDT201805005258 granted by "Fondation pour la recherche médicale (FRM)". France-BioImaging infrastructure network is supported by the French National Research Agency (ANR-10–INSB–04, Investments for the future). The use of the Opera Phenix system in the PBI core facility has been made possible by the kind financial support of the Institut Pasteur (Paris) and the Région Ile-de-France (program DIM1Health). The authors declare no conflict of interest.

AUTHORS CONTRIBUTIONS

Conception, administration, and supervision of the project: CW.
Investigation: DB, IS, and CW.
Methodology: IS, DB and PE.
Data analysis: DB, IS, PE and CW.
Visualization: DB.
Validation: IS, DB and CW.
Resources: FVP.
Funding acquisition: CW and IGB.
DB and IS wrote the original draft, under CW's supervision.
All authors contributed to the review of the manuscript and approved it for submission.

REFERENCES

1. Costa F, Hagan JE, Calcagno J, Kane M, Torgerson P, Martinez-Silveira MS, et al. Global Morbidity and Mortality of Leptospirosis: A Systematic Review. PLoS Negl Trop Dis. 2015;9(9):e0003898. Epub 20150917. doi: 10.1371/journal.pntd.0003898. PubMed PMID: 26379143; PubMed Central PMCID: PMCPMC4574773.
2. Adler B. History of leptospirosis and leptospira. Curr Top Microbiol Immunol. 2015;387:1-9. doi: 10.1007/978-3-662-45059-8_1. PubMed PMID: 25388129.
3. Ko AI, Goarant C, Picardeau M. Leptospira: the dawn of the molecular genetics era for an emerging zoonotic pathogen. Nat Rev Microbiol. 2009;7(10):736-47. doi: 10.1038/nrmicro2208. PubMed PMID: 19756012; PubMed Central PMCID: PMCPMC3384523.
4. Ratet G, Veyrier FJ, Fanton d'Andon M, Kammerscheit X, Nicola MA, Picardeau M, et al. Live imaging of bioluminescent leptospira interrogans in mice reveals renal colonization as a stealth escape from the blood defenses and antibiotics. PLoS Negl Trop Dis. 2014;8(12):e3359. Epub 20141204. doi: 10.1371/journal.pntd.0003359. PubMed PMID: 25474719; PubMed Central PMCID: PMCPMC4256284.
5. Werts C, Tapping RI, Mathison JC, Chuang TH, Kravchenko V, Saint Girons I, et al. Leptospiral lipopolysaccharide activates cells through a TLR2-dependent mechanism. Nat Immunol. 2001;2(4):346-52. doi: 10.1038/86354. PubMed PMID: 11276206.
6. Hsu SH, Hung CC, Chang MY, Ko YC, Yang HY, Hsu HH, et al. Active Components of Leptospira Outer Membrane Protein LipL32 to Toll-Like Receptor 2. Sci Rep. 2017;7(1):8363. Epub 20170821. doi: 10.1038/s41598-017-08743-y. PubMed PMID: 28827637; PubMed Central PMCID: PMCPMC5566480.
7. Ratet G, Santecchia I, Fanton d'Andon M, Vernel-Pauillac F, Wheeler R, Lenormand P, et al. LipL21 lipoprotein binding to peptidoglycan enables Leptospira interrogans to escape NOD1 and NOD2 recognition. PLoS Pathog. 2017;13(12):e1006725. Epub 20171206. doi: 10.1371/journal.ppat.1006725. PubMed PMID: 29211798; PubMed Central PMCID: PMCPMC5764436.
8. Holzapfel M, Bonhomme D, Cagliero J, Vernel-Pauillac F, Fanton d'Andon M, Bortolussi S, et al. Escape of TLR5 Recognition by Leptospira spp.: A Rationale for Atypical Endoflagella. Front Immunol. 2020;11:2007. Epub 20200811. doi: 10.3389/fimmu.2020.02007. PubMed PMID: 32849665; PubMed Central PMCID: PMCPMC7431986.
9. Murray GL, Srikram A, Henry R, Hartskeerl RA, Sermswan RW, Adler B. Mutations affecting Leptospira interrogans lipopolysaccharide attenuate virulence. Mol Microbiol. 2010;78(3):701-9. Epub 20100914. doi: 10.1111/j.1365-2958.2010.07360.x. PubMed PMID: 20807198.
10. Que-Gewirth NL, Ribeiro AA, Kalb SR, Cotter RJ, Bulach DM, Adler B, et al. A methylated phosphate group and four amide-linked acyl chains in leptospira interrogans lipid A. The membrane anchor of an unusual lipopolysaccharide that activates TLR2. J Biol Chem. 2004;279(24):25420-9. Epub 20040324. doi: 10.1074/jbc.M400598200. PubMed PMID: 15044492; PubMed Central PMCID: PMCPMC2556802.

11. Bonhomme D, Santecchia I, Vernel-Pauillac F, Caroff M, Germon P, Murray G, et al. Leptospiral LPS escapes mouse TLR4 internalization and TRIFassociated antimicrobial responses through O antigen and associated lipoproteins. PLoS Pathog. 2020;16(8):e1008639. Epub 20200813. doi: 10.1371/journal.ppat.1008639. PubMed PMID: 32790743; PubMed Central PMCID: PMCPMC7447051.

12. Lacroix-Lamande S, d'Andon MF, Michel E, Ratet G, Philpott DJ, Girardin SE, et al. Downregulation of the Na/K-ATPase pump by leptospiral glycolipoprotein activates the NLRP3 inflammasome. J Immunol. 2012;188(6):2805-14. Epub 20120208. doi: 10.4049/jimmunol.1101987. PubMed PMID: 22323544.

13. Santecchia I, Bonhomme D, Papadopoulos S, Escoll P, Giraud-Gatineau A, Moya-Nilges M, et al. Alive Pathogenic and Saprophytic Leptospires Enter and Exit Human and Mouse Macrophages With No Intracellular Replication. Front Cell Infect Microbiol 2022;12:936931. doi: doi: 10.3389/fcimb.2022.936931.

14. Sorbara MT, Ellison LK, Ramjeet M, Travassos LH, Jones NL, Girardin SE, et al. The protein ATG16L1 suppresses inflammatory cytokines induced by the intracellular sensors Nod1 and Nod2 in an autophagy-independent manner. Immunity. 2013;39(5):858-73. doi: 10.1016/j.immuni.2013.10.013. PubMed PMID: 24238340.

15. Wang Z, Li C. Xenophagy in innate immunity: A battle between host and pathogen. Dev Comp Immunol. 2020;109:103693. Epub 20200331. doi: 10.1016/j.dci.2020.103693. PubMed PMID: 32243873.

16. Travassos LH, Carneiro LA, Girardin S, Philpott DJ. Nod proteins link bacterial sensing and autophagy. Autophagy. 2010;6(3):409-11. Epub 20100426. doi: 10.4161/auto.6.3.11305. PubMed PMID: 20200479.

17. Birmingham CL, Smith AC, Bakowski MA, Yoshimori T, Brumell JH. Autophagy controls Salmonella infection in response to damage to the Salmonella-containing vacuole. J Biol Chem. 2006;281(16):11374-83. Epub 20060222. doi: 10.1074/jbc.M509157200. PubMed PMID: 16495224.

18. Gutierrez MG, Master SS, Singh SB, Taylor GA, Colombo MI, Deretic V. Autophagy is a defense mechanism inhibiting BCG and Mycobacterium tuberculosis survival in infected macrophages. Cell. 2004;119(6):753-66. doi: 10.1016/j.cell.2004.11.038. PubMed PMID: 15607973.

19. He C, Klionsky DJ. Regulation mechanisms and signaling pathways of autophagy. Annu Rev Genet. 2009;43:67-93. doi: 10.1146/annurev-genet-102808-114910. PubMed PMID: 19653858; PubMed Central PMCID: PMCPMC2831538.

20. Mizushima N, Kuma A, Kobayashi Y, Yamamoto A, Matsubae M, Takao T, et al. Mouse Apg16L, a novel WD-repeat protein, targets to the autophagic isolation membrane with the Apg12-Apg5 conjugate. J Cell Sci. 2003;116(Pt 9):1679-88. doi: 10.1242/jcs.00381. PubMed PMID: 12665549.

21. Tanida I, Ueno T, Kominami E. LC3 conjugation system in mammalian autophagy. Int J Biochem Cell Biol. 2004;36(12):2503-18. doi: 10.1016/j.biocel.2004.05.009. PubMed PMID: 15325588; PubMed Central PMCID: PMCPMC7129593.

22. Hanada T, Noda NN, Satomi Y, Ichimura Y, Fujioka Y, Takao T, et al. The Atg12-Atg5 conjugate has a novel E3-like activity for protein lipidation in autophagy. J Biol Chem. 2007;282(52):37298-302. Epub 20071106. doi: 10.1074/jbc.C700195200. PubMed PMID: 17986448.

23. Kabeya Y, Mizushima N, Ueno T, Yamamoto A, Kirisako T, Noda T, et al. LC3, a mammalian homologue of yeast Apg8p, is localized in autophagosome membranes after processing. EMBO J. 2000;19(21):5720-8. doi: 10.1093/emboj/19.21.5720. PubMed PMID: 11060023; PubMed Central PMCID: PMCPMC305793.

24. Klionsky DJ, Abdel-Aziz AK, Abdelfatah S, Abdellatif M, Abdoli A, Abel S, et al. Guidelines for the use and interpretation of assays for monitoring autophagy (4th edition)(1). Autophagy. 2021;17(1):1-382. Epub 20210208. doi: 10.1080/15548627.2020.1797280. PubMed PMID: 33634751; PubMed Central PMCID: PMCPMC7996087.

25. Xu Y, Jagannath C, Liu XD, Sharafkhaneh A, Kolodziejska KE, Eissa NT. Toll-like receptor 4 is a sensor for autophagy associated with innate immunity. Immunity. 2007;27(1):135-44. Epub 20070719. doi: 10.1016/j.immuni.2007.05.022. PubMed PMID: 17658277; PubMed Central PMCID: PMCPMC2680670.

26. Travassos LH, Carneiro LA, Ramjeet M, Hussey S, Kim YG, Magalhaes JG, et al. Nod1 and Nod2 direct autophagy by recruiting ATG16L1 to the plasma membrane at the site of bacterial entry. Nat Immunol. 2010;11(1):55-62. Epub 20091108. doi: 10.1038/ni.1823. PubMed PMID: 19898471.

27. Birmingham CL, Canadien V, Gouin E, Troy EB, Yoshimori T, Cossart P, et al. Listeria monocytogenes evades killing by autophagy during colonization of host cells. Autophagy. 2007;3(5):442-51. Epub 20070518. doi: 10.4161/auto.4450. PubMed PMID: 17568179.

28. Case ED, Chong A, Wehrly TD, Hansen B, Child R, Hwang S, et al. The Francisella O-antigen mediates survival in the macrophage cytosol via autophagy avoidance. Cell Microbiol. 2014;16(6):862-77. Epub 20131216. doi: 10.1111/cmi.12246. PubMed PMID: 24286610; PubMed Central PMCID: PMCPMC4028363.

29. Kreibich S, Emmenlauer M, Fredlund J, Ramo P, Munz C, Dehio C, et al. Autophagy Proteins Promote Repair of Endosomal Membranes Damaged by the Salmonella Type Three Secretion System 1. Cell Host Microbe. 2015;18(5):527-37. doi: 10.1016/j.chom.2015.10.015. PubMed PMID: 26567507.

30. Chen Z, Wang T, Liu Z, Zhang G, Wang J, Feng S, et al. Inhibition of Autophagy by MiR-30A Induced by Mycobacteria tuberculosis as a Possible Mechanism of Immune Escape in Human Macrophages. Jpn J Infect Dis. 2015;68(5):420-4. Epub 20150410. doi: 10.7883/yoken.JJID.2014.466. PubMed PMID: 25866116.

31. Choy A, Dancourt J, Mugo B, O'Connor TJ, Isberg RR, Melia TJ, et al. The Legionella effector RavZ inhibits host autophagy through irreversible Atg8 deconjugation. Science. 2012;338(6110):1072-6. Epub 20121025. doi: 10.1126/science.1227026. PubMed PMID: 23112293; PubMed Central PMCID: PMCPMC3682818.

32. Ogawa M, Yoshimori T, Suzuki T, Sagara H, Mizushima N, Sasakawa C. Escape of intracellular Shigella from autophagy. Science. 2005;307(5710):727-31. Epub 20041202. doi: 10.1126/science.1106036. PubMed PMID: 15576571.

33. Manzanillo PS, Ayres JS, Watson RO, Collins AC, Souza G, Rae CS, et al. The ubiquitin ligase parkin mediates resistance to intracellular pathogens. Nature. 2013;501(7468):512-6. Epub 20130904. doi: 10.1038/nature12566. PubMed PMID: 24005326; PubMed Central PMCID: PMCPMC3886920.

34. Mostowy S, Sancho-Shimizu V, Hamon MA, Simeone R, Brosch R, Johansen T, et al. p62 and NDP52 proteins target intracytosolic Shigella and Listeria to different autophagy pathways. J Biol Chem. 2011;286(30):26987-95. Epub 20110606. doi: 10.1074/jbc.M111.223610. PubMed PMID: 21646350; PubMed Central PMCID: PMCPMC3143657.

35. Watson RO, Bell SL, MacDuff DA, Kimmey JM, Diner EJ, Olivas J, et al. The Cytosolic Sensor cGAS Detects Mycobacterium tuberculosis DNA to Induce Type I Interferons and Activate Autophagy. Cell Host Microbe. 2015;17(6):811-9. Epub 20150602. doi: 10.1016/j.chom.2015.05.004. PubMed PMID: 26048136; PubMed Central PMCID: PMCPMC4466081.

36. Zheng YT, Shahnazari S, Brech A, Lamark T, Johansen T, Brumell JH. The adaptor protein p62/SQSTM1 targets invading bacteria to the autophagy pathway. J Immunol. 2009;183(9):5909-16. Epub 20091007. doi: 10.4049/jimmunol.0900441. PubMed PMID: 19812211.

37. Wlodarska M, Thaiss CA, Nowarski R, Henao-Mejia J, Zhang JP, Brown EM, et al. NLRP6 inflammasome orchestrates the colonic host-microbial interface by regulating goblet cell mucus secretion. Cell. 2014;156(5):1045-59. doi: 10.1016/j.cell.2014.01.026. PubMed PMID: 24581500; PubMed Central PMCID: PMCPMC4017640.

38. Jounai N, Kobiyama K, Shiina M, Ogata K, Ishii KJ, Takeshita F. NLRP4 negatively regulates autophagic processes through an association with beclin1. J Immunol. 2011;186(3):1646-55. Epub 20110105. doi: 10.4049/jimmunol.1001654. PubMed PMID: 21209283.

39. Deng Q, Wang Y, Zhang Y, Li M, Li D, Huang X, et al. Pseudomonas aeruginosa Triggers Macrophage Autophagy To Escape Intracellular Killing by Activation of the NLRP3 Inflammasome. Infect Immun. 2016;84(1):56-66. Epub 20151014. doi: 10.1128/IAI.00945-15. PubMed PMID: 26467446; PubMed Central PMCID: PMCPMC4694000.

40. Lai M, Yao H, Shah SZA, Wu W, Wang D, Zhao Y, et al. The NLRP3-Caspase 1 Inflammasome Negatively Regulates Autophagy via TLR4-TRIF in Prion Peptide-Infected Microglia. Front Aging Neurosci. 2018;10:116. Epub 20180418. doi: 10.3389/fnagi.2018.00116. PubMed PMID: 29720937; PubMed Central PMCID: PMCPMC5915529.

41. Jain A, Lamark T, Sjottem E, Larsen KB, Awuh JA, Overvatn A, et al. p62/SQSTM1 is a target gene for transcription factor NRF2 and creates a positive feedback loop by inducing antioxidant response element-

driven gene transcription. J Biol Chem. 2010;285(29):22576-91. Epub 20100507. doi: 10.1074/jbc.M110.118976. PubMed PMID: 20452972; PubMed Central PMCID: PMCPMC2903417.

42. Komatsu M, Kurokawa H, Waguri S, Taguchi K, Kobayashi A, Ichimura Y, et al. The selective autophagy substrate p62 activates the stress responsive transcription factor Nrf2 through inactivation of Keap1. Nat Cell Biol. 2010;12(3):213-23. Epub 20100221. doi: 10.1038/ncb2021. PubMed PMID: 20173742.

43. Lau A, Wang XJ, Zhao F, Villeneuve NF, Wu T, Jiang T, et al. A noncanonical mechanism of Nrf2 activation by autophagy deficiency: direct interaction between Keap1 and p62. Mol Cell Biol. 2010;30(13):3275-85. Epub 20100426. doi: 10.1128/MCB.00248-10. PubMed PMID: 20421418; PubMed Central PMCID: PMCPMC2897585.

44. Kong X, Thimmulappa R, Craciun F, Harvey C, Singh A, Kombairaju P, et al. Enhancing Nrf2 pathway by disruption of Keap1 in myeloid leukocytes protects against sepsis. Am J Respir Crit Care Med. 2011;184(8):928-38. Epub 20110728. doi: 10.1164/rccm.201102-0271OC. PubMed PMID: 21799073; PubMed Central PMCID: PMCPMC3208662.

45. Kobayashi EH, Suzuki T, Funayama R, Nagashima T, Hayashi M, Sekine H, et al. Nrf2 suppresses macrophage inflammatory response by blocking proinflammatory cytokine transcription. Nat Commun. 2016;7:11624. Epub 20160523. doi: 10.1038/ncomms11624. PubMed PMID: 27211851; PubMed Central PMCID: PMCPMC4879264.

46. Abby SS, Cury J, Guglielmini J, Neron B, Touchon M, Rocha EP. Identification of protein secretion systems in bacterial genomes. Sci Rep. 2016;6:23080. Epub 20160316. doi: 10.1038/srep23080. PubMed PMID: 26979785; PubMed Central PMCID: PMCPMC4793230.

47. Nahori MA, Fournie-Amazouz E, Que-Gewirth NS, Balloy V, Chignard M, Raetz CR, et al. Differential TLR recognition of leptospiral lipid A and lipopolysaccharide in murine and human cells. J Immunol. 2005;175(9):6022-31. doi: 10.4049/jimmunol.175.9.6022. PubMed PMID: 16237097.

48. Bonhomme D, Hernandez-Trejo V, Papadopoulos S, Pigache R, Fanton d'Andon M, Outlia A, et al. *Leptospira interrogans* prevents macrophage cell death and pyroptotic IL1ß releasethrough atypical lipopolysaccharide. BioRXiv. doi: 10.1101/2022.07.25.501344.

49. Terawaki S, Camosseto V, Prete F, Wenger T, Papadopoulos A, Rondeau C, et al. RUN and FYVE domain-containing protein 4 enhances autophagy and lysosome tethering in response to Interleukin-4. J Cell Biol. 2015;210(7):1133-52. doi: 10.1083/jcb.201501059. PubMed PMID: 26416964; PubMed Central PMCID: PMCPMC4586740.

50. Ye X, Zhu M, Che X, Wang H, Liang XJ, Wu C, et al. Lipopolysaccharide induces neuroinflammation in microglia by activating the MTOR pathway and downregulating Vps34 to inhibit autophagosome formation. J Neuroinflammation. 2020;17(1):18. Epub 20200111. doi: 10.1186/s12974-019-1644-8. PubMed PMID: 31926553; PubMed Central PMCID: PMCPMC6954631.

51. Yin S, Cao W. Toll-Like Receptor Signaling Induces Nrf2 Pathway Activation through p62-Triggered Keap1 Degradation. Mol Cell Biol. 2015;35(15):2673-83. Epub 20150526. doi: 10.1128/MCB.00105-15. PubMed PMID: 26012548; PubMed Central PMCID: PMCPMC4524114.

52. Jiang T, Harder B, Rojo de la Vega M, Wong PK, Chapman E, Zhang DD. p62 links autophagy and Nrf2 signaling. Free Radic Biol Med. 2015;88(Pt B):199-204. Epub 20150624. doi: 10.1016/j.freeradbiomed.2015.06.014. PubMed PMID: 26117325; PubMed Central PMCID: PMCPMC4628872.

53. Gilardini Montani MS, Santarelli R, Granato M, Gonnella R, Torrisi MR, Faggioni A, et al. EBV reduces autophagy, intracellular ROS and mitochondria to impair monocyte survival and differentiation. Autophagy. 2019;15(4):652-67. Epub 20181023. doi: 10.1080/15548627.2018.1536530. PubMed PMID: 30324853; PubMed Central PMCID: PMCPMC6526866.

54. Bichiou H, Rabhi S, Ben Hamda C, Bouabid C, Belghith M, Piquemal D, et al. Leishmania Parasites Differently Regulate Antioxidant Genes in Macrophages Derived From Resistant and Susceptible Mice. Front Cell Infect Microbiol. 2021;11:748738. Epub 20211015. doi: 10.3389/fcimb.2021.748738. PubMed PMID: 34722338; PubMed Central PMCID: PMCPMC8554229.

55. Zavala-Alvarado C, Sismeiro O, Legendre R, Varet H, Bussotti G, Bayram J, et al. The transcriptional response of pathogenic Leptospira to peroxide reveals new defenses against infection-related oxidative stress. PLoS Pathog. 2020;16(10):e1008904. Epub 20201006. doi: 10.1371/journal.ppat.1008904. PubMed PMID: 33021995; PubMed Central PMCID: PMCPMC7567364.

56. Vivarini AC, Calegari-Silva TC, Saliba AM, Boaventura VS, Franca-Costa J, Khouri R, et al. Systems Approach Reveals Nuclear Factor Erythroid 2-Related Factor 2/Protein Kinase R Crosstalk in Human Cutaneous Leishmaniasis. Front Immunol. 2017;8:1127. Epub 20170915. doi: 10.3389/fimmu.2017.01127. PubMed PMID: 28959260; PubMed Central PMCID: PMCPMC5605755.

57. Macoch M, Morzadec C, Genard R, Pallardy M, Kerdine-Romer S, Fardel O, et al. Nrf2-dependent repression of interleukin-12 expression in human dendritic cells exposed to inorganic arsenic. Free Radic Biol Med. 2015;88(Pt B):381-90. Epub 20150211. doi: 10.1016/j.freeradbiomed.2015.02.003. PubMed PMID: 25680285.

58. Helou DG, Braham S, De Chaisemartin L, Granger V, Damien MH, Pallardy M, et al. Nrf2 downregulates zymosan-induced neutrophil activation and modulates migration. PLoS One. 2019;14(8):e0216465. Epub 20190816. doi: 10.1371/journal.pone.0216465. PubMed PMID: 31419224; PubMed Central PMCID: PMCPMC6697320.

59. Fanton d'Andon M, Quellard N, Fernandez B, Ratet G, Lacroix-Lamande S, Vandewalle A, et al. Leptospira Interrogans induces fibrosis in the mouse kidney through Inos-dependent, TLR- and NLR-independent signaling pathways. PLoS Negl Trop Dis. 2014;8(1):e2664. Epub 20140130. doi: 10.1371/journal.pntd.0002664. PubMed PMID: 24498450; PubMed Central PMCID: PMCPMC3907306.

60. Raffray L, Giry C, Vandroux D, Kuli B, Randrianjohany A, Pequin AM, et al. Major Neutrophilia Observed in Acute Phase of Human Leptospirosis Is Not Associated with Increased Expression of Granulocyte Cell Activation Markers. PLoS One. 2016;11(11):e0165716. Epub 20161101. doi: 10.1371/journal.pone.0165716. PubMed PMID: 27802348; PubMed Central PMCID: PMCPMC5089758.

61. Olagnier D, Brandtoft AM, Gunderstofte C, Villadsen NL, Krapp C, Thielke AL, et al. Nrf2 negatively regulates STING indicating a link between antiviral sensing and metabolic reprogramming. Nat Commun. 2018;9(1):3506. Epub 20180829. doi: 10.1038/s41467-018-05861-7. PubMed PMID: 30158636; PubMed Central PMCID: PMCPMC6115435.

62. Werts C, le Bourhis L, Liu J, Magalhaes JG, Carneiro LA, Fritz JH, et al. Nod1 and Nod2 induce CCL5/RANTES through the NF-kappaB pathway. Eur J Immunol. 2007;37(9):2499-508. doi: 10.1002/eji.200737069. PubMed PMID: 17705131.

63. Santecchia I, Vernel-Pauillac F, Rasid O, Quintin J, Gomes-Solecki M, Boneca IG, et al. Innate immune memory through TLR2 and NOD2 contributes to the control of Leptospira interrogans infection. PLoS Pathog. 2019;15(5):e1007811. Epub 20190520. doi: 10.1371/journal.ppat.1007811. PubMed PMID: 31107928; PubMed Central PMCID: PMCPMC6544334.

64. Bonhomme D, Werts C. Purification of LPS from Leptospira. Methods Mol Biol. 2020;2134:53-65. doi: 10.1007/978-1-0716-0459-5_6. PubMed PMID: 32632859.

FIGURES LEGENDS

Figure 1. *L. interrogans* reduces the quantity of autophagosomes in macrophages

A) WB of LC3 in C57/BL6 mouse peritoneal cells 4 h post-intraperitoneal injection of PBS, 5 x 10^7 *L. interrogans* serovar Manilae strain MFLum1 (*L.i*), 30 µg of muropeptides (murP) (MDP+FK156) or 30 µg of rapamycin (Rap). **B)** WB of LC3 in BMDMs 24 h post-infection with either live or heat-killed (HK) *L. interrogans* serovar Manilae strain MFLum1 at MOI 100, or stimulation with 500 nM rapamycin. **C)** WB of LC3 in BMDMs 24 h post-infection with *L. interrogans* serovar Manilae strain MFLum1 at MOI 100, with or without bafilomycin A1 (BafA1) addition 4 h before cell collection. **D)** WB analyses and quantifications of LC3 in BMDMs 1 h, 4 h and 24 h post-infection with either live or HK *L. interrogans* serovar Manilae strain MFLum1 at MOI 100. Quantifications represent the ratio of LC3-II in stimulated cells over non-stimulated cells, and after stain free normalization. Each dot corresponds to the quantification of a blot from an independent experiment (*n* from 3 to 6). **E)** RT-qPCR analyses of LC3 mRNA levels in BMDMs 24 h post-infection with MOI 100 of *L. interrogans* serovar Manilae strain L495. Bars correspond to mean +/- SD of technical replicates (*n*=4). **F-G)** High Content (HC) confocal microscopy images and quantifications of RAW-mLC3-DiFluo cells 4 h post-infection with *L. interrogans* serovar Manilae strain MFLum1 at MOI 100, with or without bafilomycin A1 (BafA1) addition 2 h before cell fixation. Bars correspond to mean +/- SD of technical replicates (*n*=4). **A-E)** Data presented are representative of at least 3 independent experiments.

Figure 2. *L. interrogans* induces specific accumulation of p62 adaptor in puncta-like structures

A) WB of p62 in BMDMs 1 h, 4 h and 24 h post-infection with *L. interrogans* serovar Manilae strain MFLum1. **B)** WB of p62 in BMDMs 24 h post-infection with *L. interrogans* serovar Manilae strain MFLum1, serovar Copenhageni strain Fiocruz L1-130, serovar Icterohaemorrhagiae strain Verdun, and *L. biflexa* serovar Patoc strain Patoc I. **C)** RT-qPCR analyses of p62 mRNA levels in BMDMs 24 h post-infection with *L. interrogans* serovar Manilae strain L495. Bars correspond to mean +/- SD of technical replicates (*n*=4). **D)** Epifluorescence analyses of p62 in BMDMs 4 h post-infection with *L. interrogans* serovar Manilae strain MFLum1. **E)** High Content (HC) confocal microscopy analyses of the number of p62 puncta *per* cell and the percentage of p62 positive cells 1 h, 4 h and 24 h post-infection of RAW264.7 cells with *L. interrogans* serovar Manilae strain L495. **F)** HC single cell microscopy analysis of the number of p62 puncta *per* cell 24 h post-infection of RAW264.7 cells with *L. interrogans* serovar Manilae strain L495. **A-F)** Data presented are representative of at least 3 independent experiments.

Figure 3. Autophagy modulation is mediated by TLR2/TLR4

A) WB of LC3 and p62 in WT and TLR2/4 dko BMDMs 24 h post-infection with *L. interrogans* serovar Manilae strain MFLum1 at MOI 100, or upon starvation induction by incubation in EBSS medium. **B)** WB of p62 in WT and MyD88/TRIF dko BMDMs 24 h post-infection with *L. interrogans* serovar Manilae strain MFLum1. **C)** RT-qPCR analyses of p62 mRNA levels in WT and TLR2/4 dko BMDMs 24 h post-infection with *L. interrogans* serovar Manilae strain L495 at MOI 100. Bars correspond to mean of independent experiments (*n*=3). **D)** High Content (HC) single cell microscopy analysis of the number of p62 puncta *per* cell 24 h post-infection of WT, TLR2/TLR4 dko and

MyD88/TRIF dko BMDMs with *L. interrogans* serovar Manilae strain L495, serovar Copenhageni strain Fiocruz L1-130 and serovar Icterohaemorrhagiae strain Verdun. **A-D)** Data presented are representative of at least 2 independent experiments.

Figure 4. p62 accumulation is mediated by the leptospiral LPS

A) WB of p62 in BMDMs 1 h, 4 h and 24 h post-stimulation with heat-killed (56°C, 30 min) *L. interrogans* serovar Manilae strain MFLum1 at MOI 100 or 24 h post-stimulation with 1 µg/mL of the corresponding purified leptospiral LPS. **B)** High Content (HC) confocal microscopy analyses of the number of p62 puncta *per* cell and the percentage of p62 positive cells 1 h, 4 h and 24 h post-stimulation of RAW264.7 cells with MOI 100 of either live or heat-killed (56°C, 30 min) *L. interrogans* serovar Manilae strain L495 or stimulation with 1 µg/mL of the corresponding purified leptospiral LPS. **C)** HC single cell microscopy analysis of the number of p62 puncta *per* cell 24 h post-infection of RAW264.7 cells with MOI 100 of either live or heat-killed (56°C, 30 min) *L. interrogans* serovar Manilae strain L495 or stimulation with 1 µg/mL of the corresponding purified leptospiral LPS. **A-C)** Data presented are representative of at least 3 independent experiments.

Figure 5. Leptospiral LPS also triggers translocation of NRF2 transcription factor

A) Confocal microscopy analyses of NRF2 in BMDMs 4 h post-infection with *L. interrogans* serovar Manilae strain L495 at MOI 100. **B)** High Content (HC) single cell microscopy analysis of the levels of NRF2 intensity in the nucleus and 4 h post-infection of RAW264.7 cells with *L. interrogans* serovar Manilae strain L495, serovar Copenhageni strain Fiocruz L1-130 or serovar Icterohaemorrhagiae strain Verdun, at MOI 100. Fluorescence is expressed in arbitrary units (AU), dashed lines correspond to median. **C)** HC analysis of the number of cells with NRF2 intensity ratio [nucleus/cytoplasm] > 1.4 4 h post-infection of RAW264.7 cells with *L. interrogans* serovar Manilae strain L495, serovar Copenhageni strain Fiocruz L1-130 or serovar Icterohaemorrhagiae strain Verdun, at MOI 100. **D)** HC single cell microscopy analysis of the levels of NRF2 intensity in the nucleus 4 h post-infection of RAW264.7 cells with MOI 100 of either live or heat-killed (56°C, 30 min) *L. interrogans* serovar Manilae strain L495 or stimulation with 1 µg/mL of the corresponding purified leptospiral LPS. Fluorescence is expressed in arbitrary units (AU), dashed lines correspond to median. **E)** HC analysis of the number of cells with NRF2 intensity ratio [nucleus/cytoplasm] > 1.4 4 h post-infection of RAW264.7 cells with MOI 100 of either live or heat-killed (56°C, 30 min) *L. interrogans* serovar Manilae strain L495 or stimulation with 1 µg/mL of the corresponding purified leptospiral LPS. **A-E)** Data presented are representative of at least 2 independent experiments.

Figure 6. p62 and NRF2 constitute a retro-activation loop upon infection with *L. interrogans*

A) High Content (HC) single cell microscopy analysis of NRF2 intensity ratio [nucleus/cytoplasm] in BMDMs transfected with scramble (scrbl) or p62 siRNA and infected for 4 h with *L. interrogans* serovar Manilae strain L495 at MOI 100. **B)** Corresponding controls are microscopy analyses and quantification of p62 intensity in the same transfection and infection conditions. Lines correspond to mean +/- SD of technical replicates (n=3). **C)** HC single cell microscopy analysis of p62 puncta formation in BMDMs transfected with scrbl or NRF2 siRNA and infected for 4 h with *L. interrogans* serovar Manilae strain L495 at MOI 100. **D)** Corresponding controls are microscopy analyses and quantification of NRF2 intensity in the same transfection and infection conditions. Lines correspond to mean +/- SD of technical replicates (n=3). **E)** WB of p62 in BMDMs transfected with scrbl or NRF2

siRNA and infected for 24 h with *L. interrogans* serovar Manilae strain L495 at MOI 10 or 100. **F)** RT-qPCR analyses of p62 mRNA levels in RAW264.7 cells transfected with scrbl or NRF2 siRNA and infected for 24 h with *L. interrogans* serovar Manilae strain L495 at MOI 100. Bars correspond to mean of independent experiments (*n*=2). **A-E)** Data presented are representative of at least 3 independent experiments.

Figure 7. NRF2 translocation prevents inflammation upon infection

A) Cell viability (measured by MTT assay) and **B)** LDH release (measured by CyQuant assay) in RAW264.7 cells transfected with scramble (scrbl) or NRF2 siRNA and infected for 24 h with *L. interrogans* serovar Manilae strain L495 at MOI 100. Bars correspond to mean +/- SD of technical replicates (*n*=4). **B)** RT-qPCR analyses of iNOS, IL6, TNF and IL10 mRNA levels in RAW264.7 cells transfected with scrbl or NRF2 siRNA and infected for 10 h with *L. interrogans* serovar Manilae strain L495 at MOI 100. Bars correspond to mean of independent experiments (*n*=3). **C)** NO dosage by Griess reaction and, IL6, TNF and IL10 by ELISA in RAW264.7 cells transfected with scrbl or NRF2 siRNA and infected for 24 h with *L. interrogans* serovar Manilae strain L495 at MOI 100. Bars correspond to mean +/- SD of technical replicates (*n*=4). **A-C)** Data presented are representative of at least 3 independent experiments.

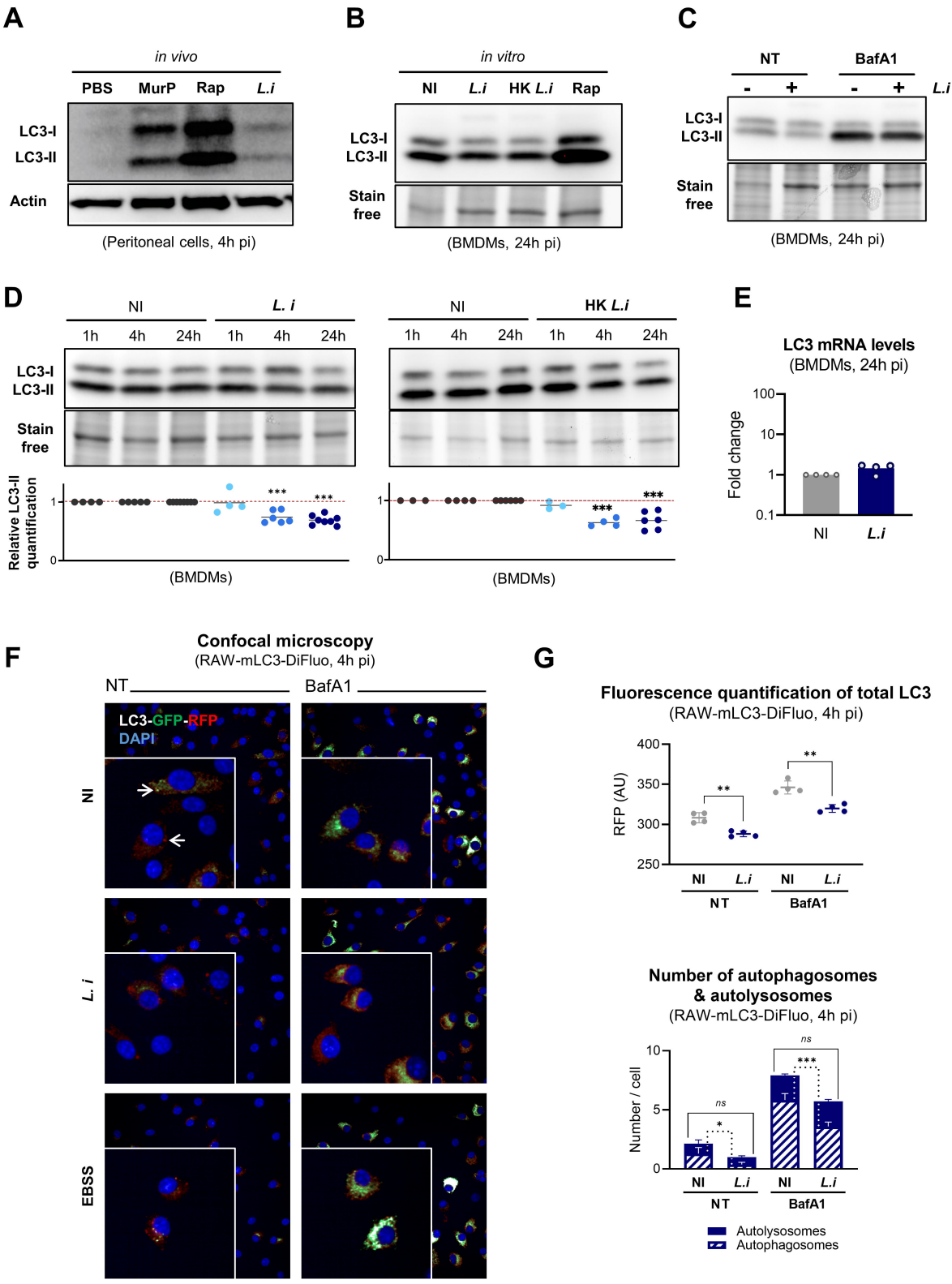
A
in vivo
PBS
MurP
Rap
L.i
LC3-I
LC3-II
Actin
(Peritoneal cells, 4h pi)
B
in vitro
NI
L.i
HK L.i
Rap
LC3-I
LC3-II
Stain free
(BMDMs, 24h pi)
C
NT
BafA1
-
+
-
+
L.i
LC3-I
LC3-II
Stain free
(BMDMs, 24h pi)
D
NI
L. i
1h
4h
24h
1h
4h
24h
LC3-I
LC3-II
Stain free
Relative LC3-II quantification
1
0
***
***
(BMDMs)
NI
HK L.i
1h
4h
24h
1h
4h
24h
1
0
***
***
(BMDMs)
E
LC3 mRNA levels
(BMDMs, 24h pi)
Fold change
100
10
1
0.1
NI
L.i
F
Confocal microscopy
(RAW-mLC3-DiFluo, 4h pi)
NT
BafA1
LC3-GFP-RFP
DAPI
NI
L. i
EBSS
G
Fluorescence quantification of total LC3
(RAW-mLC3-DiFluo, 4h pi)
RFP (AU)
400
350
300
250
**
**
NI
L.i
NI
L.i
NT
BafA1
Number of autophagosomes
& autolysosomes
(RAW-mLC3-DiFluo, 4h pi)
Number / cell
10
5
0
ns
*
ns
***
NI
L.i
NI
L.i
NT
BafA1
Autolysosomes
Autophagosomes

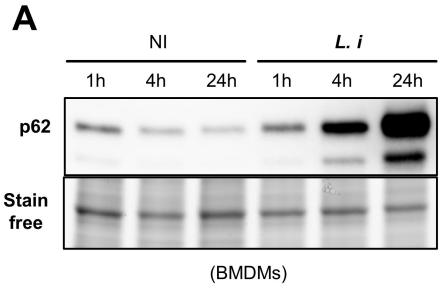
A
NI
L. i
1h
4h
24h
1h
4h
24h
p62
Stain free
(BMDMs)

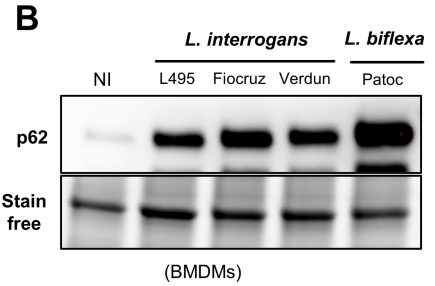
B
L. interrogans
L. biflexa
NI
L495
Fiocruz
Verdun
Patoc
p62
Stain free
(BMDMs)

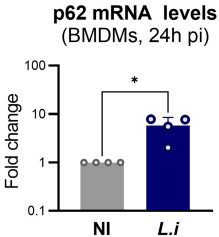
C
p62 mRNA levels
(BMDMs, 24h pi)
Fold change
100
10
1
0.1
*
NI
L.i

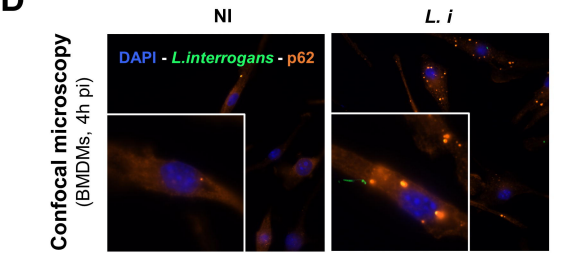
D
NI
L. i
Confocal microscopy
(BMDMs, 4h pi)
DAPI - L.interrogans - p62

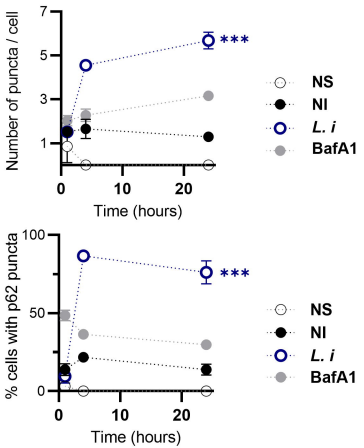
E
Kinetics of p62 puncta formation
(RAW264.7)
Number of puncta / cell
7
5
3
1
***
0
10
20
Time (hours)
NS
NI
L. i
BafA1
% cells with p62 puncta
100
50
0
***
0
10
20
Time (hours)
NS
NI
L. i
BafA1

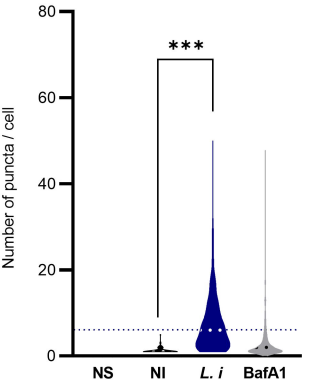
F
Single cell analysis of p62 puncta
(RAW264.7, 24h pi)
Number of puncta / cell
80
60
40
20
0
***
NS
NI
L. i
BafA1

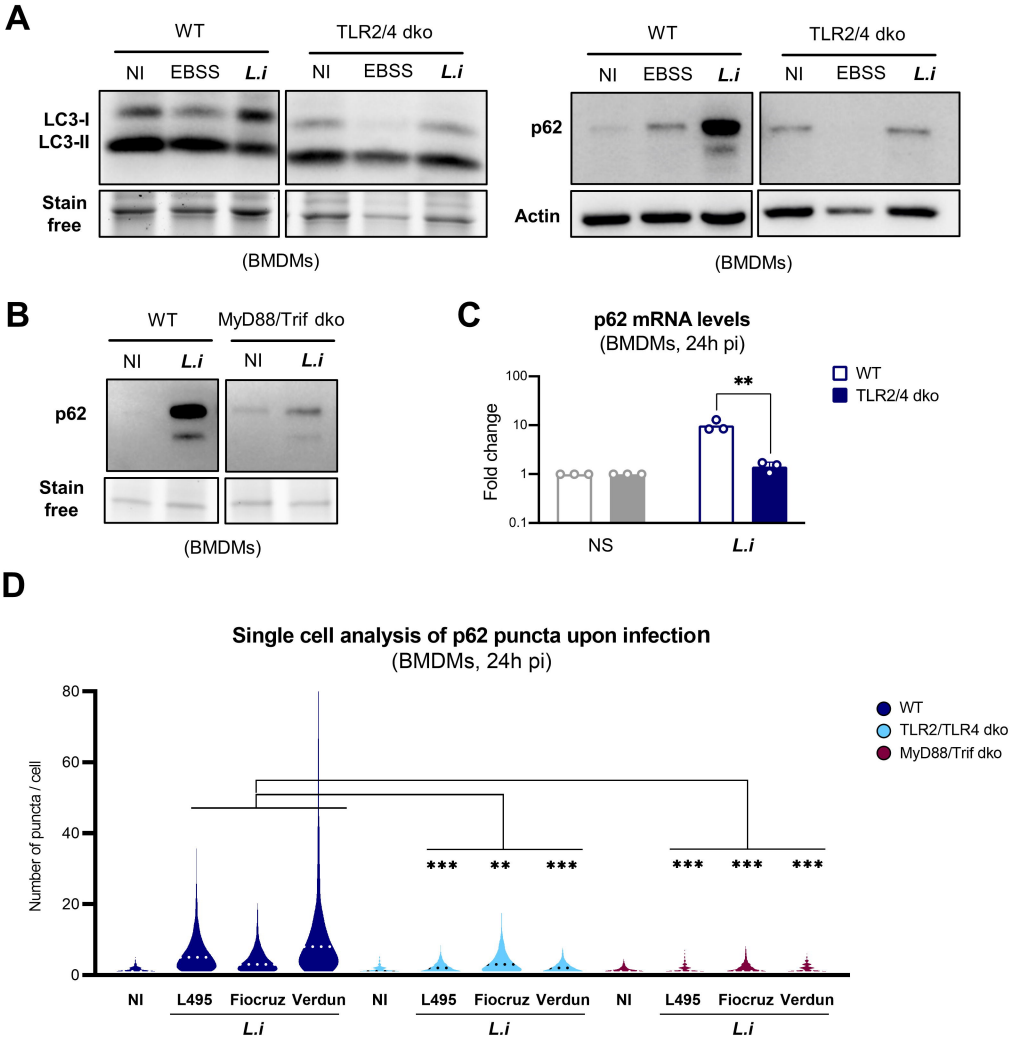
A
WT
TLR2/4 dko
NI
EBSS
L.i
LC3-I
LC3-II
Stain free
(BMDMs)
p62
Actin
B
MyD88/Trif dko
C
p62 mRNA levels
(BMDMs, 24h pi)
Fold change
100
10
1
0.1
**
NS
D
Single cell analysis of p62 puncta upon infection
Number of puncta / cell
80
60
40
20
0
L495
Fiocruz
Verdun
TLR2/TLR4 dko
MyD88/Trif dko
***

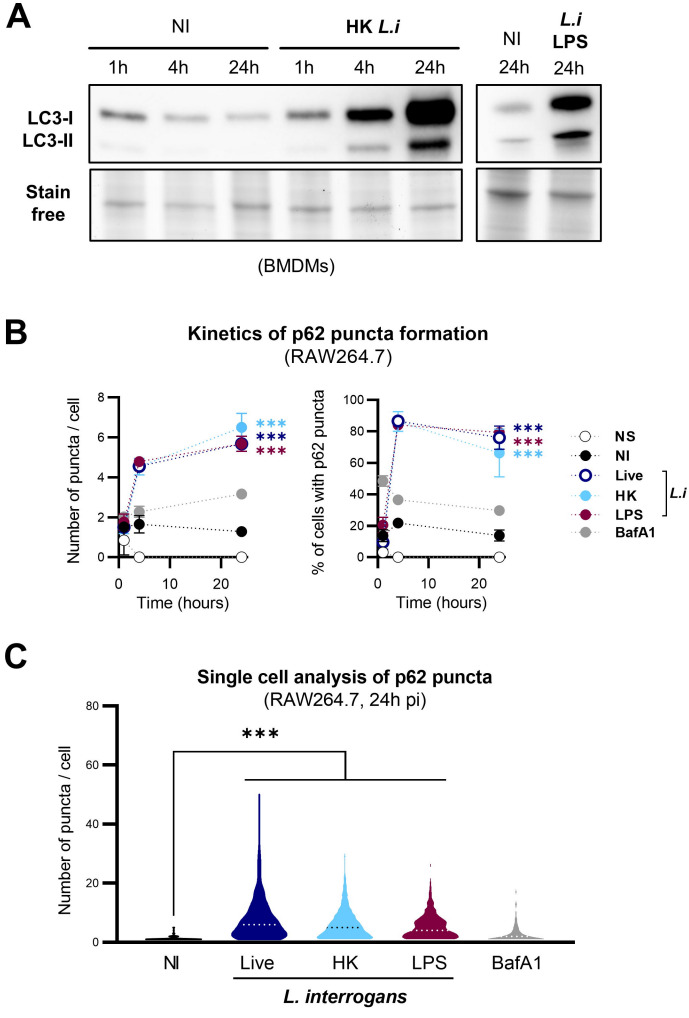
A
NI
HK L.i
NI
L.i LPS
1h
4h
24h
1h
4h
24h
24h
24h
LC3-I
LC3-II
Stain free
(BMDMs)
B
Kinetics of p62 puncta formation
(RAW264.7)
Number of puncta / cell
Time (hours)
% of cells with p62 puncta
Time (hours)
***
NS
NI
Live
HK
LPS
BafA1
L.i
C
Single cell analysis of p62 puncta
(RAW264.7, 24h pi)
Number of puncta / cell
***
NI
Live
HK
LPS
BafA1
L. interrogans

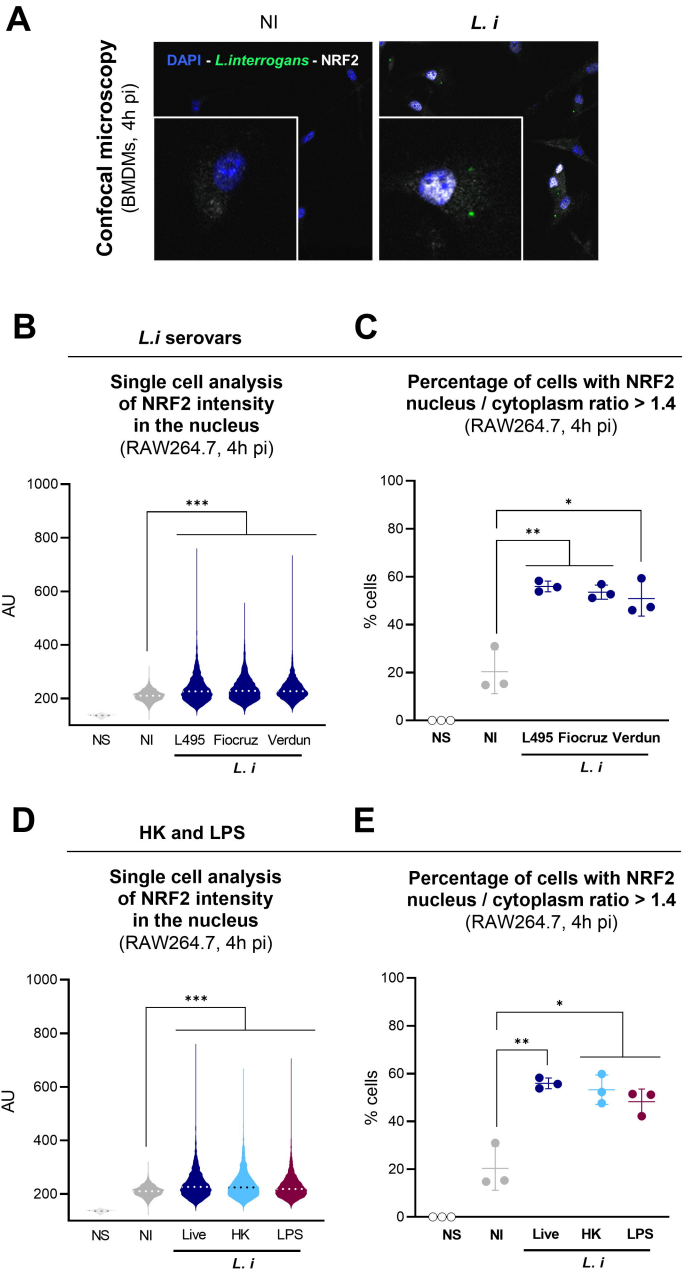
A
NI
L. i
Confocal microscopy
(BMDMs, 4h pi)
DAPI - L.interrogans - NRF2
B
L.i serovars
Single cell analysis
of NRF2 intensity
in the nucleus
(RAW264.7, 4h pi)
AU
1000
800
600
400
200
***
NS
NI
L495
Fiocruz
Verdun
L. i
C
Percentage of cells with NRF2
nucleus / cytoplasm ratio > 1.4
(RAW264.7, 4h pi)
% cells
100
80
60
40
20
0
*
**
NS
NI
L495
Fiocruz
Verdun
L. i
D
HK and LPS
Single cell analysis
of NRF2 intensity
in the nucleus
(RAW264.7, 4h pi)
AU
1000
800
600
400
200
***
NS
NI
Live
HK
LPS
L. i
E
Percentage of cells with NRF2
nucleus / cytoplasm ratio > 1.4
(RAW264.7, 4h pi)
% cells
100
80
60
40
20
0
*
**
NS
NI
Live
HK
LPS
L. i

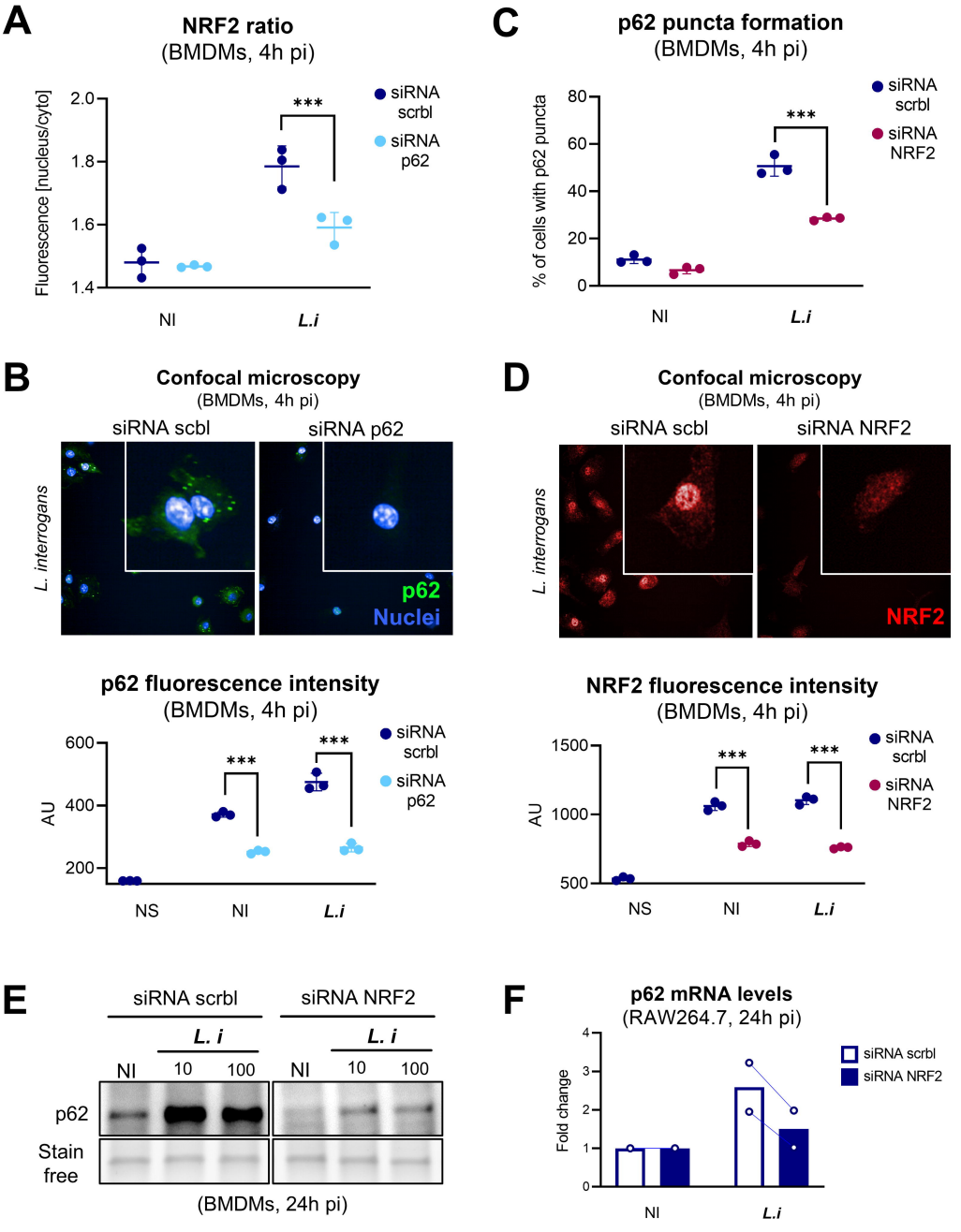
A
NRF2 ratio
(BMDMs, 4h pi)
Fluorescence [nucleus/cyto]
2.0
1.8
1.6
1.4
***
siRNA scrbl
siRNA p62
NI
L.i
C
p62 puncta formation
(BMDMs, 4h pi)
% of cells with p62 puncta
80
60
40
20
0
***
siRNA scrbl
siRNA NRF2
NI
L.i
B
Confocal microscopy
(BMDMs, 4h pi)
siRNA scbl
siRNA p62
L. interrogans
p62
Nuclei
D
Confocal microscopy
(BMDMs, 4h pi)
siRNA scbl
siRNA NRF2
L. interrogans
NRF2
p62 fluorescence intensity
(BMDMs, 4h pi)
AU
600
400
200
***
***
siRNA scrbl
siRNA p62
NS
NI
L.i
NRF2 fluorescence intensity
(BMDMs, 4h pi)
AU
1500
1000
500
***
***
siRNA scrbl
siRNA NRF2
NS
NI
L.i
E
siRNA scrbl
siRNA NRF2
L. i
L. i
NI
10
100
NI
10
100
p62
Stain free
(BMDMs, 24h pi)
F
p62 mRNA levels
(RAW264.7, 24h pi)
Fold change
4
3
2
1
0
siRNA scrbl
siRNA NRF2
NI
L.i

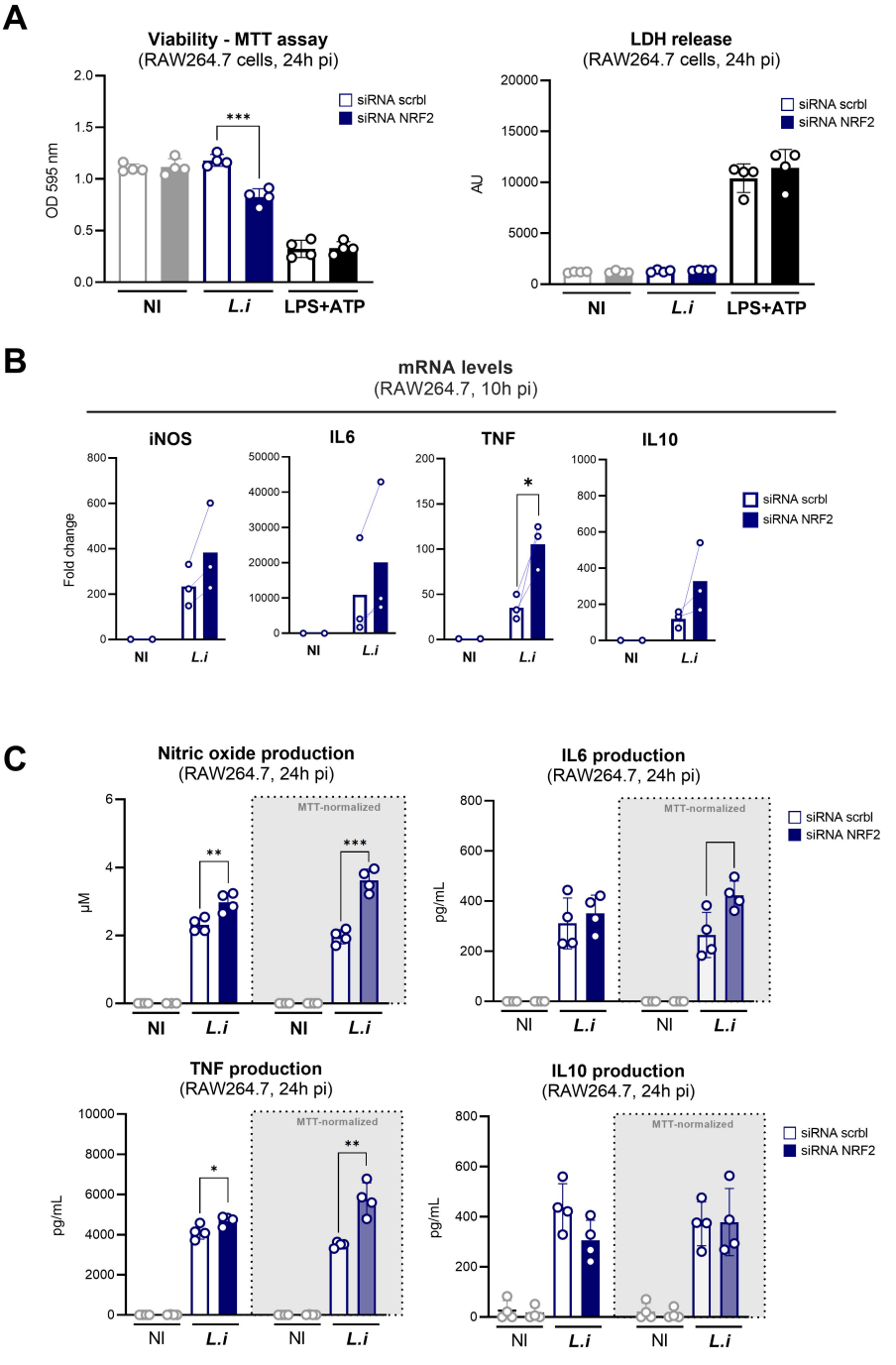
A
Viability - MTT assay
(RAW264.7 cells, 24h pi)
OD 595 nm
2.0
1.5
1.0
0.5
0.0
***
siRNA scrbl
siRNA NRF2
NI
L.i
LPS+ATP
LDH release
(RAW264.7 cells, 24h pi)
AU
20000
15000
10000
5000
0
B
mRNA levels
(RAW264.7, 10h pi)
iNOS
IL6
TNF
IL10
Fold change
*
C
Nitric oxide production
(RAW264.7, 24h pi)
µM
MTT-normalized
**
***
IL6 production
(RAW264.7, 24h pi)
pg/mL
TNF production
(RAW264.7, 24h pi)
IL10 production
(RAW264.7, 24h pi)